JCTC Journal of Chemical Theory and Computation

Article

pubs.acs.org/JCTC

Development of Accurate DFT Methods for Computing Redox Potentials of Transition Metal Complexes: Results for Model Complexes and Application to Cytochrome P450

Thomas F. Hughes and Richard A. Friesner*

Department of Chemistry, Columbia University, New York, New York 10027, United States

Supporting Information

ABSTRACT: Single-electron reduction half potentials of 95 octahedral fourth-row transition metal complexes binding a diverse set of ligands have been calculated at the unrestricted pseudospectral B3LYP/LACV3P level of theory in a continuum solvent. Through systematic comparison of experimental and calculated potentials, it is determined that B3LYP strongly overbinds the d-manifold when the metal coordinates strongly interacting ligands and strongly underbinds the d-manifold when the metal coordinates weakly interacting ligands. These error patterns give rise to an extension of the localized orbital correction (LOC) scheme previously developed for organic molecules and which was recently extended to the spin-splitting properties of organometallic complexes. Mean unsigned errors in B3LYP redox potentials are reduced from 0.40 ± 0.20 V (0.88 V max error) to 0.12 ± 0.09 V (0.34 V max error) using a simple seven-parameter model. Although the focus of this article is on redox properties of transition metal complexes, we have found that applying our previous spin-splitting LOC model to an independent test set of oxidized and reduced complexes that are also spin-crossover complexes correctly reverses the ordering of spin states obtained with B3LYP. Interesting connections are made between redox and spin-splitting parameters with regard to the spectrochemical series and in their combined predictive power for properly closing the thermodynamic cycle of d-electron transitions in a transition metal complex. Results obtained from our large and diverse databases of spin-splitting and redox properties suggest that, while the error introduced by single reference B3LYP for simple multireference systems, like mononuclear transition metal complexes, remains significant, at around 2−5 kcal/mol, the dominant error, at around 10−20 kcal/mol, is in B3LYP's prediction of metal−ligand binding. Application of the LOC scheme to the rate-determining hydrogen atom transfer step in substrate hydroxylation by cytochrome P450 shows that this approach is able to correct the B3LYP barriers in comparison to recent kinetics experiments.

1. INTRODUCTION

Chemical reactions that take place in important materials science and biochemical applications often involve electron transfer or proton coupled electron transfer events in solution, for example, redox reactions between reducing (electron donor) and oxidizing (electron acceptor) species, that in many cases are rate-determining.[1−7] Redox reactions are essentially inseparable from the study of chemical reactions involving transition metals where the metal center can typically adopt various oxidation states which give rise to the possibility of multiple reactive channels with different activation barriers. Depending on the nature of the ligands and the specific redox couple, the reduction can induce a facile spin-crossover due to the reduced formal oxidation state of the metal and the resulting decrease in the magnitude of the ligand field splitting parameter, Δ_o.[8,9] To quickly and accurately investigate the mechanisms of electrochemical reactions involving transition metals and/or to design new complexes with specific redox properties etc. calls for better quantum chemical methods for modeling redox reactions.

Without resorting to high-level multireference *ab initio* quantum chemistry methods, which can be prohibitively expensive for the kinds of studies needed in common biochemical and materials science applications, the development of a parametrized model that can accurately predict redox potentials of transition metal complexes necessitates a detailed understanding of the underlying electronic structure and energetics of the d-manifold. The magnitudes and signs of the redox potentials from a database of complexes can appear quite different from one another due to the unique HOMO/LUMO energetics which are determined by the strength of the ligand field and the resulting shift in d orbitals relative to the free metal center. As is well known from basic molecular orbital theory, the HOMO/LUMO orbitals are energy eigenstates that can be delocalized and thus are formally represented as a linear combination of localized orbitals. In the absence of a chromophore, electron removal and/or attachment from/to the HOMO/LUMO orbitals are in fact removals and/or attachments of fractional electron contributions summed over a potentially very large number of localized orbitals. In this article, the word chromophore retains its traditional meaning as a region of a molecule which is responsible for the color of that molecule but for which the definition is relaxed to include light that is outside of the visible range. Thus the chromophore represents a region of the molecule whose local energetic changes due to a change in electronic state are essentially decoupled from the remainder of the molecule. In the case of a relatively strong chromophore, as in the metal centers of the complexes from the redox database discussed below, the ionization is localized to the

Received: September 23, 2011
Published: January 13, 2012

 © 2012 American Chemical Society dx.doi.org/10.1021/ct2006693 | J. Chem. TheoryComput. 2012, 8, 442−459

metal center with only small fractional electron contributions from the ligands.

Redox models have been proposed on the basis of the principle of ligand additivity[10−17] where the potential of a given complex can be predicted by summing ligand parameters from a ligand electrochemical series. Ligand additivity is a good assumption provided that the ligands are only weakly interacting with one another and provides a way to predict how the HOMO/LUMO orbital energies will shift under ligand substitution. Models due to Pickett et al.,[13,14] Bursten et al.,[15,16] and Lever[17] are some of the more common ligand additivity models, and electronic structure calculations, specifically Fenske−Hall[18] and more recently DFT,[19] have been used to investigate various proposed electrochemical series. A recent review is offered by Pombeiro.[20] Series are derived from experimental redox potentials, typically starting from simple cases like low spin octahedral homoleptic complexes with large ligand field splitting energies resulting from either strongly interacting ligands which lie to the far right of the spectrochemical series or large central metal atomic numbers as in transition metals from the fifth and sixth rows of the periodic table. For example, Lever's model[17] begins with a very large systematic set of experimental Ru(III/II) redox couples from the literature. For a series of complexes of the form $[M(L)_n(L')_{6-n}]^{+q}$ and the conversion of $[M(L)_6]^{+q_1}$ to $[M(L')_6]^{+q_2}$ where L and L′ are ligands with different electron affinities, the redox potentials are found to be linearly correlated with n as in the following equation:

$$E^o_{1/2}([M(L)_n(L')_{6-n}]^{+q}) = \frac{n}{6}E^o_{1/2}([M(L)_6]^{+q_1}) + \frac{(6-n)}{6}E^o_{1/2}([M(L')_6]^{+q_2}) \quad (1)$$

Total redox potentials are modeled in Lever's approach,[17] and thus a new parameter set must be introduced for each new electronic structure, for example depending on the metal center, oxidation state, and whether the reduction is low spin to low spin, high spin to high spin, low spin to high spin, etc. The database that Lever has constructed deserves special recognition because it is by far among the largest of its kind and thus is able to reveal other patterns in the electronic structure; for example, in certain cases like those that involve fifth- and sixth-row metals like Nb,[17] Tc,[21] and Re,[22] successive redox couples share the same Lever slope parameter, which under certain assumptions would allow the prediction of all couples for a given complex with the knowledge of any single couple.

The manners in which these ligand electrochemical series are used to predict redox potentials of transition metal complexes are similar to how other well-known series in organic and inorganic chemistry are used, for example, the series of Hammett constants,[23,24] which is used to predict inductive effects and thus reactivity of molecules containing aromatic rings with substituents, and the spectrochemical series, which is used to predict the ligand field splitting parameter and determine the ground state multiplicity of a given transition metal complex. Exact interpretation of differences in ligand ordering between the different electrochemical series and the spectrochemical series is not clear due to uncertainties present in the experimental and calculated data. For example, the ordering of many of the ligands is conserved between the series with the notable exception of the cyano ligand, which is believed to be due to π-backbonding.[17]

Despite the fact that our redox model will necessarily make use of the systematic behavior of the HOMO/LUMO orbitals across a variety of transition metal complexes, it is significantly different from the ligand additivity models discussed above, most notably because we are interested in describing the error patterns of B3LYP[25,26] with respect to experimental results as opposed to a highly parametrized model that targets total redox potentials. In this article, we investigate the single-electron redox properties of a diverse database of 95 octahedral fourth-row transition metal complexes using the B3LYP functional. By systematically isolating errors in the B3LYP redox potentials with respect to experimental results, a previously determined localized orbital correction (LOC) scheme for transition metal complexes, d-block LOC (DBLOC),[27] can be extended to reproduce the experimental potentials by using a small number of additional parameters. Original work on the LOC scheme has shown that for organic molecules the errors in B3LYP are predominantly localizable to individual valence bonds and their static or "in−out" electron correlation contributions.[28] The LOC scheme has since been extended to various equilibrium and nonequilibrium properties of organic molecules[29−31] and was more recently extended to the calculation of metal atoms[32] and spin-splitting properties of transition metal complexes.[27] In the latter, spin-splittings for the following types of electronic transitions, i.e. $t_{2g} \rightarrow t_{2g}$, $e_g \rightarrow e_g$, $t_{2g} \rightarrow e_g$, or $e_g \rightarrow t_{2g}$, were corrected using a five parameter LOC model that was fit to a diverse database of 57 experimental spin-forbidden transition energies for fourth-row octahedral transition metal complexes. These parameters were found to correlate with the spectrochemical series and provided an accuracy of 1.98 ± 1.62 kcal/mol compared to the 10.14 ± 4.56 kcal/mol error in conventional B3LYP. This article serves as an extension of the LOC scheme for transition metal complexes to enable the calculation of redox potentials to a similar level of accuracy and which when combined with the previous spin-splitting parameter set provides a general model for treating a variety of different spin state and electronic transitions in the d manifold. For these transition-metal-containing problems, the physical interpretation of the B3LYP errors remains quite similar to that originally proposed for organic molecules;[28] for example, in the case of spin-splitting properties, as well as the redox properties presented below, B3LYP makes errors in the static correlation components to the pairing of electrons in the d manifold as well as in the interactions that bind the ligands to the metal.

Several publications have investigated redox calculations of transition metal complexes using DFT,[8,11,33−41] and they show different levels of success. For example, one of the earliest studies provided by Baik and Friesner[36] shows reasonable errors of about 100−200 mV with larger errors seen in certain cases, while a recent paper by Batista et al.[33] shows that some functionals can be in error by 500 mV, and even by as much as 900 mV, for carbonyl bound complexes and metallocenes involving fourth-, fifth-, and sixth-row metal centers. Despite their success in calculating the properties of systems composed of organic molecules, DFT methods may encounter many difficulties for organometallic systems due to both the possibility of poor physics in the underlying wave function and simply a poor understanding of the wave function itself. Some specific issues with DFT for transition metal complexes are (1) the choice of functional and basis set which, for spin-crossover complexes or other complexes with low-lying excited states, can change the ground state multiplicity; (2) incorrect representation of the electron density necessary to bind the metal and ligand, which we have found can produce unphysical redox noninnocence where the ligands act as the chromophores and

dx.doi.org/10.1021/ct2006693 | J. Chem. TheoryComput. 2012, 8, 442−459

the electron removal and/or attachment process becomes predominantly localized to the ligands for situations where the valence ionizations are supposed to be localized to the metal center; (3) multireference aspects which are formally unavoidable by virtue of the single determinant ansatz of DFT; and (4) SCF convergence issues and sensitivity to the initial guess wave function, which can converge the DFT wave function to an excited state and make the comparison of properties for similar complexes appear to be noisy and unsystematic even though they are not. Due to the large space of chemical descriptors for transition metal complexes, e.g., oxidation state, multiplicity, coordination type and number, etc., as well as experimental and computational sources of uncertainty, it is difficult to benchmark the performance of DFT without resorting to very large and diverse databases of transition metal complexes.

We have found that many of these problems, with the exception of fixing the actual energetics, which is reserved for our empirical LOC scheme, can be addressed by using a series of initial guess wave functions, discussed at great length in previous work,[27,42] that properly sample different electron configurations in the d manifold and ultimately provide a better signal-to-noise ratio over the database. In previous work, DFT calculations were found to be particularly sensitive to the initial guess wave functions when calculating the spin-splitting energies of transition metal complexes. We have found that similar sampling is needed for spin-crossover coupled redox reactions. For the computation of redox potentials in the commonly encountered situation, where both oxidized and reduced forms are in their electronic ground states with large gaps to the nearest excited states, low values of the keyword *istate* (see the Methods section of this article or previous references[27,42] for a more detailed discussion) typically produce the correct ground state multiplicity, although there are exceptions to this rule.

In the Methods section, we first discuss the creation and content of our database of redox properties for transition metal complexes, placing some emphasis on the different types of spin-crossover complexes present in the database, as well as provide a brief summary of the protocol used in our calculations and redox solvation model. For more details on the calculation protocol, the reader is referred to our previous article on spin-splittings.[27] In the Results and Discussion section, we first discuss our assignments of ground state electronic structures for the oxidized and reduced complexes in our database and how the principle of ligand additivity applies to some interesting families of complexes. We then summarize the redox data for all 95 complexes and discuss the effects due to exact nonlocal exchange in the B3LYP functional as well as the correlation with the spectrochemical series. The final DBLOC model is given in subsection 3.3.3, and the connections between redox and spin-splitting parameters are discussed in subsection 3.3.4. Finally, in section 4, we apply the model to the hydrogen atom abstraction reaction performed by cytochrome P450.

2. METHODS

2.1. Redox Database. Initial attempts to create a database of experimental electrochemical properties for transition metal complexes included a number of different published studies, each of which mainly focused on a single type of complex. This made it difficult to assess the quality of the redox potentials calculated with B3LYP due to both computational and experimental sources of uncertainty. Examples of the latter include possible solvent coordination, redox noninnocence, reactive couples, poor knowledge of reference potentials in different solvents,[43] etc. Other sources of noise have been discussed by Lever.[17] Therefore, in constructing our database, we maximized the number of published results in which more systematic series of experiments were performed, for example, as in series of complexes where the metal remains the same and the ligand is varied or vice versa. We began with an initial understanding of the B3LYP error patterns, in particular with regard to the electronic structure of the metal center, which was then supplemented with the aforementioned publications that focused on a single type of complex. Unlike our previous spin-splitting database, for which it was quite difficult to find a diverse set of experiments, there are a very large number of publications on the redox properties of transition metal complexes, and so while our database is both large and diverse, it is obviously not exhaustive. This provided an initial database containing the experimental redox potentials of 110 complexes; however, due to additional sources of both experimental and computational errors and uncertainties, which are discussed in Table 1 of the Results and Discussion section, as well as other computational difficulties, 15 complexes were removed from the initial database, resulting in the final redox database of 95 complexes which is used throughout this article.

The systematic experimental studies included in our redox database are for series of complexes in which a number of different metal centers are bound to each type of ligand from the following list: cyano, $(C_5(CH_3)_5)^{-1}$ (cpstar), tacn, tpen, tp, acac, water, cl4bdt, edta, and cdta, and slightly smaller systematic studies were included for terpy, phen, bpy, nap, cit, ox, mnt, and pdt. The ligands in the database range from small and mono-dentate to large and hexa-dentate. For convenience, they are named either by common abbreviations used in the literature or from condensed empirical formulas. The structures of the ligands can be seen in the complexes shown in the Supporting Information. This diverse set of ligands is representative of transition metal environments encountered in materials science and biochemistry applications. The database includes six Ti, seven V, 20 Cr, 12 Mn, 24 Fe, 19 Co, and seven Ni complexes ranging from singlet to sextet multiplicities and with total charges and total numbers of d electrons ranging from −4 to 3 and from 0 to 8, respectively. All redox reactions are single-electron metal-centered reductions of octahedral mononuclear fourth-row transition metal complexes found in the following set of references: refs 8, 33, 36, 44−75. Typically, it is the III/II redox couple that was experimentally measured in either water (ε = 80.4), acetonitrile (ε = 37.5), or dichloromethane (ε = 9.1) solvents. To the best of our knowledge, these redox reactions are not coupled to proton transfer.

For experimental studies that did not report the spin states of the complexes involved in a given redox couple, we have determined the ground state multiplicities of the oxidized and reduced forms of the complex by either (1) comparison with experiments performed on similar systems with known ground states, (2) using the spectrochemical series and other rules concerning the magnitude of Δ_o from basic inorganic chemistry, or (3) using B3LYP/LACV3P, which is reliable for determining the ground state multiplicities of transition metal complexes provided that they are not spin-crossover complexes. About 10% of the complexes in our redox database exhibit spin-crossover behavior, and for these complexes, our previous spin-splitting DBLOC model is used to provide the correct ground state multiplicities. A description of the application of DBLOC to these spin-crossover complexes can be found in section 3.1 of the Results and Discussion section. In this redox database, there are also spin-crossover coupled redox reactions that

Table 1. Transition Metal Complexes That Were Initially in the Redox Database but Were Removed Due to Various Complications in the Experiments, Calculations, or Possibly Both Experiment and Calculation

complex	reference	description
$[Mn(III)(cdta)]^{-1}$	*Inorg. Chem.* **1967**, *6*, 139	The experiment suggests that this complex likely binds a water molecule.
$[Mn(III)(edta)]^{-1}$	*Inorg. Chem.* **1967**, *6*, 139	The experiment suggests that this complex likely binds a water molecule.
$[Ti(IV)(dtpa)]^{+1}$	*J. Inorg. Biochem.* **2010**, *104*, 1006	By comparison with experimental and calculated results for the other Ti(IV) and Fe(III) complexes presented in this article, it appears, based on a very large outlier in the exptl. − calcd. redox error, that there is something wrong with either the experimental or calculated redox potentials for the $[Ti(IV)(dtpa)]^{+1}$ complex.
$[Fe(III)(dtpa)]$	*J. Inorg. Biochem.* **2010**, *104*, 1006	This complex was removed because the only other complex involving the dtpa ligand, $[Ti(IV)(dtpa)]^{+1}$, was removed.
$[Cr(IV)(dmhp)_3]^{+1}$	*Synth. React. Inorg., Met.-Org., Nano-Met. Chem.* **2005**, *35*, 61	The experiment suggests that this species has organized solvent, and the calculations predict noninnocent ligands and suffer from large spin contamination.
$[Cr(IV)(ma)_3]^{+1}$	*Synth. React. Inorg., Met.-Org., Nano-Met. Chem.* **2005**, *35*, 61	Calculations predict noninnocent ligands and suffer from large spin contamination.
$[Co(III)(nh3)_6]^{+3}$	*Tables of Standard Electrode Potentials*; John Wiley and Sons: New York, 1978	Calculations suggest that the sign of the experimental redox potential reported in the reference provided may be incorrect.
$[Co(III)(en)_3]^{+3}$	*Standard Potentials in Aqueous Solution*; IUPAC: Zurich, Switzerland, 1985	Originally, the experimental redox potential for this complex was recorded as 0.18 V and was attributed to experimental error; however, later after the complex was removed, it was discovered that the potential was −0.18 V.
$[Cr(III)(nh3)_6]^{+3}$	*Inorg. Chim. Acta* **1992**, *194*, 15	The results for this complex give a very large outlier in the exptl. − calcd. error, and we are not certain why this complex presents difficulties.
$[Mn(IV)(tp)_2]^{+2}$	*Inorg. Chem.* **2003**, *42*, 3616	Although we have a few examples of complexes with multiple redox potentials in our redox database, for example, a few of the complexes with coordinating sulfurs, we have not yet attempted to develop a model for such cases because it would require an extensive database of such cases, and so we eliminated $[Mn(IV)(tp)_2]^{+2}$ due to an insufficient number of other similar complexes
$[Ni(III)(dapo)_2]^{-1}$	*J. Am. Chem. Soc.* **1990**, *112*, 2955	The calculations predict noninnocent ligands.
$[Ni(III)(pspyr)_2]^{+3}$	*Inorg. Chem.* **1994**, *33*, 4869	The calculations suffer from some spin contamination, and we saw no point of including the new phosphorus atom type without more reliable calculations.
$[Cr(III)(pic)_3]$	*Z. Anorg. Allg. Chem.* **2003**, *629*, 1085	The calculations suffer from large spin contamination.
$[Ni(III)(pscoo)_2]^{+1}$	*Inorg. Chem.* **1994**, *33*, 4869	The calculations suffer from some spin contamination, and we saw no point of including the new phosphorus atom type without more reliable calculations.
$[Cr(III)(cyclam)(h2o)_2]^{+3}$	*Inorg. Chim. Acta* **1992**, *194*, 15	The calculations predict noninnocent ligands.

manifest in two specific ways: (1) a number of Mn(III) complexes (eighth row of Table 2 from the Results and Discussion section) undergoing reduction show spin-crossover behavior as in the $t_{2g}^2 t_{2g}^1 t_{2g}^1 e_g^0 e_g^0 \rightarrow t_{2g}^1 t_{2g}^1 t_{2g}^1 e_g^1 e_g^1$ reaction, and (2) a number of Co(III) complexes (15th row of Table 2) undergoing reduction show spin-crossover behavior as in the $t_{2g}^2 t_{2g}^2 t_{2g}^2 e_g^0 e_g^0 \rightarrow t_{2g}^2 t_{2g}^2 t_{2g}^1 e_g^1 e_g^1$ reaction. At high temperatures, a Fe(III) couple can also show this type of spin-crossover coupled reduction as in the $t_{2g}^2 t_{2g}^2 t_{2g}^1 e_g^0 e_g^0 \rightarrow t_{2g}^2 t_{2g}^1 t_{2g}^1 e_g^1 e_g^1$ reaction. Our previous spin-splitting DBLOC model is also used here to correct the spin-crossover component of the error in spin-crossover coupled redox reactions. Specific applications of DBLOC to the spin-crossover coupled redox reactions can be found in section 3.3.3 of the Results and Discussion section. It is important to distinguish this type of spin-crossover reaction, where the redox reaction is coupled to spin-crossover and involves an increase of three in the number of unpaired electrons in going from the oxidized to the reduced forms of the complex, from the aforementioned cases where either the oxidized or reduced complexes are spin-crossover complexes for which the number of unpaired electrons changes by only ±1 upon reduction.

2.2. Calculation Protocol. Geometry optimizations and single point calculations were performed using Jaguar version 7.5[76] with the relativistic effective core potential LACV3P, which is a triple-ζ contraction of the LACVP[77] basis set, for metal centers and 6-311G for the rest of the atoms. While the B3LYP spin-splitting properties of transition metal complexes studied in our previous article showed only a small dependence on basis set, for example, less than 1 kcal/mol difference in the spin-splittings calculated using the basis sets LACV3P, LACV3P++**, and LACV3P+/6-311G-3df-3pd, there is greater dependence on basis set for the B3LYP redox properties. For example, the B3LYP redox potentials can change by as much as 0.4 V depending on the electronic structure of the transition metal complexes involved in the redox couple, and while increasing the size of the basis set can improve the agreement with experimental results in some cases, in other cases it resulted in poorer agreement with experimental results. Upon changing to a larger basis set, we do expect some changes in our final set of redox parameters; however, we do not expect a qualitative change in the underlying physical model. The parametrization presented here should be viewed as basis set specific; however, it should be relatively straightforward to construct parameters of approximately equal efficacy for other basis sets.

Redox potentials were determined from adiabatic ΔSCF methods using fully unrestricted pseudospectral B3LYP free energies of the oxidized and reduced complexes. The standard reduction half potential, $E_{1/2}^o$, is related to the standard electron attachment (EA) free energy of solvation, ΔG_{EA}^{o36}, by

$$\Delta G_{EA}{}^o = G^o(A^-) - G^o(A) = \Delta G_{1/2}{}^o = -FE_{1/2}{}^o \quad (2)$$

where solvation superscripts are assumed throughout, F is the Faraday constant, and A is the oxidized form of the complex. Redox

dx.doi.org/10.1021/ct2006693 | J. Chem. TheoryComput. 2012, 8, 442−459

Table 2. Ligand Field Diagrams for the Oxidized and Reduced Forms of All of the Transition Metal Complexes in the Redox Database Including Spin-Crossover Complexes and Spin-Crossover Coupled Redox Reactions

complex	oxidized	reduced
$[Ti(IV)(nap)_3]^{-2}$, $[Ti(IV)(cit)_3]^{-2}$, $[Ti(IV)(cl4bdt)_3]^{-2}$, $[V(V)(pdt)_3]^{+1}$, $[Ti(IV)(hbed)]$, $[Ti(IV)(edta)]$, $[Ti(IV)(cdta)]$	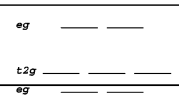	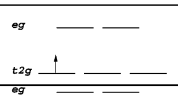
$[V(IV)(cl4bdt)_3]^{-2}$, $[V(IV)(mnt)_3]^{-2}$, $[V(IV)(pdt)_3]^{-2}$	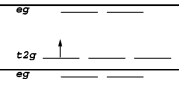	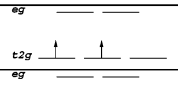
$[V(III)(acac)_3]$, $[Cr(IV)(cl4bdt)_3]^{-2}$, $[V(III)(mnt)_3]^{-3}$, $[V(III)(edta)]^{-1}$	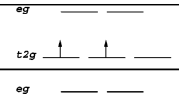	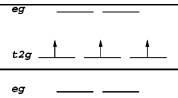
$[Cr(III)(cn)_6]^{-3}$, $[Cr(III)(phen)_3]^{+3}$, $[Cr(III)(bpy)_3]^{+3}$, $[Cr(III)(cyclam)(cn)_2]^{+1}$, $[Cr(III)(en)_2(cn)_2]^{+1}$	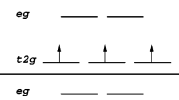	
$[Cr(III)(cpstar)_2]^{+1}$, $[Cr(III)(tpen)]^{+3}$, $[Cr(III)(tp)_2]^{+1}$	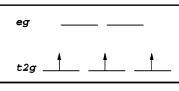	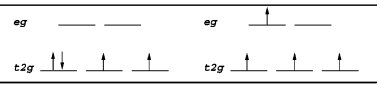
$[Cr(III)(tacn)_2]^{+3}$, $[Cr(III)(en)_3]^{+3}$, $[Cr(III)(en)_2(ncs)_2]^{+1}$, $[Cr(III)(acac)_3]$, $[Cr(III)(h2o)_6]^{+3}$, $[Mn(IV)(cl4bdt)_3]^{-2}$, $[Cr(III)(edta)]^{-1}$, $[Cr(III)(cdta)]^{-1}$, $[Cr(III)(mida)_2]^{-1}$, $[Cr(III)(cl)(l15)]^{+2}$, $[Cr(III)(cyclam)(cl)_2]^{+1}$		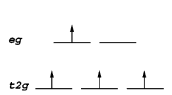
$[Mn(III)(cn)_6]^{-3}$, $[Mn(III)(cn)_5(no)]^{-2}$	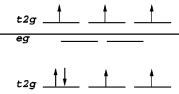	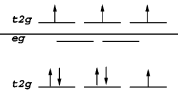
$[Mn(III)(cpstar)_2]^{+1}$, $[Mn(III)(tacn)_2]^{+3}$, $[Mn(III)(tpen)]^{+3}$, $[Mn(III)(tp)_2]^{+1}$, $[Mn(III)(terpy)_2]^{+3}$, $[Mn(III)(cl)(l52)]^{+2}$	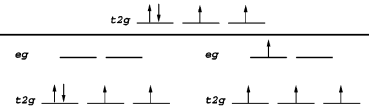	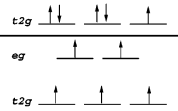
$[Mn(III)(acac)_3]$, $[Mn(III)(h2o)_6]^{+3}$, $[Mn(III)(cl4bdt)_3]^{-3}$, $[Fe(IV)(cl4bdt)_3]^{-2}$	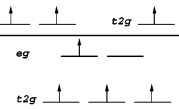	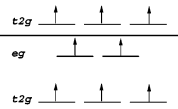
$[Fe(III)(cn)_6]^{-3}$, $[Fe(III)(phen)_3]^{+3}$, $[Fe(III)(bpy)_3]^{+3}$, $[Fe(III)(py26diox)_2]^{-1}$, $[Fe(III)(py2ox)_3]$, $[Fe(III)(bpy)_2(cn)_2]^{+1}$, $[Fe(III)(bpy)(cn)_4]^{-1}$, $[Fe(III)(cn)_5(no)]^{-2}$	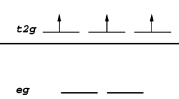	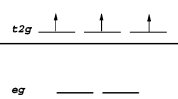
$[Fe(III)(cpstar)_2]^{+1}$, $[Fe(III)(tacn)_2]^{+3}$, $[Fe(III)(tpen)]^{+3}$, $[Fe(III)(tp)_2]^{+1}$, $[Fe(III)(terpy)_2]^{+3}$	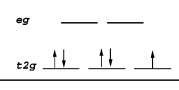	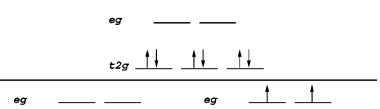
$[Fe(III)(nap)_3]^{-3}$, $[Fe(III)(cit)_3]^{-3}$, $[Fe(III)(ox)_3]^{-3}$, $[Fe(III)(acac)_3]$, $[Fe(III)(h2o)_6]^{+3}$, $[Fe(III)(cl4bdt)_3]^{-3}$, $[Fe(III)(hbed)]^{-1}$, $[Fe(III)(edta)]^{-1}$, $[Fe(III)(cdta)]^{-1}$, $[Fe(III)(cl)(l52)]^{+2}$	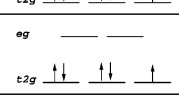	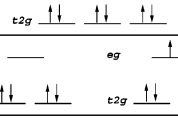
$[Co(III)(cn)_6]^{-3}$, $[Co(III)(phen)_3]^{+3}$, $[Co(III)(bpy)_3]^{+3}$, $[Cr(0)(co)_5(pycn)]$	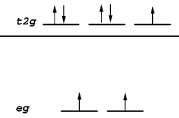	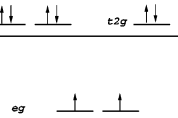
$[Co(III)(cpstar)_2]^{+1}$, $[Co(III)(tacn)_2]^{+3}$, $[Co(III)(den)_2]^{+3}$, $[Co(III)(tpen)]^{+3}$, $[Co(III)(tp)_2]^{+1}$, $[Co(III)(terpy)_2]^{+3}$	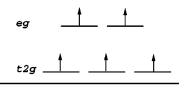	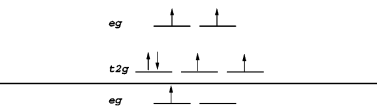
$[Co(III)(ox)_3]^{-3}$, $[Co(III)(acac)_3]$, $[Co(III)(h2o)_6]^{+3}$, $[Co(III)(ox)_2(h2o)_2]^{-1}$, $[Co(III)(edta)]^{-1}$, $[Co(III)(cdta)]^{-1}$, $[Co(III)(pdta)]^{-1}$, $[Co(III)(h2o)_4(phen)]^{+3}$, $[Co(III)(gly)_3]$, $[Co(III)(h2o)_2(phen)_2]^{+3}$	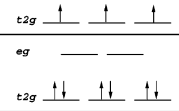	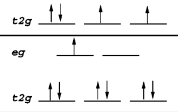
$[Ni(III)(cpstar)_2]^{+1}$, $[Ni(III)(tacn)_2]^{+3}$, $[Ni(III)(tpen)]^{+3}$, $[Ni(III)(tp)_2]^{+1}$, $[Ni(III)(s2cnet2)_3]$, $[Ni(III)(edta)]^{-1}$, $[Ni(III)(pdtc)_2]^{-1}$	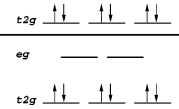	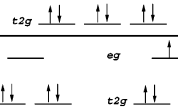

potentials are reported relative to the experimental normal hydrogen electrode (NHE) reference potential of 4.44 V. In this article, units of volts (V) have been used which are energy (eV) per unit electron charge (e). The Cambridge Structural Database[78] was used to obtain the initial geometries of most complexes. Spin−orbit corrections were not included because for fourth-row transition metal complexes their effects are typically small.[41] As recently discussed at great length,[27,42] initial guess density matrices are used which sample different electronic configurations of the metal[79] and help to alleviate some of the difficulties that quantum chemical methods have with convergence to the correct states of transition metal complexes.

2.3. Solvation Model. The Poisson−Boltzmann solver in Jaguar[76] has been used to provide a continuum dielectric model of the solvents used in the experiments, either water, acetonitrile, or dichloromethane. The default atomic radii provided in

dx.doi.org/10.1021/ct2006693 | J. Chem. TheoryComput. 2012, 8, 442−459

Jaguar[76] have been used. We saw only small differences between redox potentials computed in water (ε = 80.4) and acetonitrile (ε = 37.5) even for highly charged redox couples like $[Fe(III)(tpen)]^{+3}$, for which the B3LYP/LACV3P error with respect to experiment decreases from 0.56 to 0.43 V as we change from water to acetonitrile, which is the solvent used in the experiment. Comparing redox potentials calculated in water with those calculated in dichloromethane (ε = 9.1) we saw small differences for couples with small total charges, for example, as in $[Ni(III)(cpstar)_2]^{+1}$, where the error increases from −0.70 V to −0.88 V as we change from water to dichloromethane, which is the solvent used in the experiment. Larger differences were seen for couples with larger total charges, for example, as in the $[Fe(III)(cl4bdt)_3]^{-3}$ complex where the error decreases substantially from −1.17 V to −0.26 V as we change from water to dichloromethane, which is the solvent used in the experiment. These results show the importance of including solvation effects in modeling the redox properties of transition metal complexes, especially in the case of a highly charged couple in a weak dielectric medium where we found that using the incorrect solvent changed the calculated potential by 0.91 V. A detailed discussion of the dependence of redox potentials on other solution conditions along with a number of figures of experimental and calculated data is provided in the Supporting Information.

3. RESULTS AND DISCUSSION

3.1. Ligand Field Diagrams. To develop the B3LYP LOC model for the redox properties of transition metal complexes, it is first necessary to determine the B3LYP electronic structures of the oxidized and reduced complexes. Ligand field diagrams for all 95 complexes in the redox database are shown in Table 2. Ligand field diagrams for metallocenes are assumed to have a two-level splitting into t_{2g} and e_g orbitals most like that of an octahedral complex, and it can be seen, for example in a recent article by Swart,[80] that this is a good approximation. For spin-crossover complexes, the convention we use is to show the low temperature ground states to the left of a given oxidized or reduced pair. As previously mentioned, for spin-crossover complexes, B3LYP provides an incorrect ordering of spin state energetics in comparison to low temperature experimental measurements, which results in a ground state of the wrong spin multiplicity. This is a result of the 20% exact nonlocal exchange in the B3LYP functional and its overstabilization of high spin states for spin-crossover complexes. In our redox database, most of the Cr(II), Mn(III), and Co(II) complexes involving the cpstar, tacn, tpen, tp, terpy, and a few other ligands are spin-crossover complexes. Ground state multiplicities of Fe(II) spin-crossover complexes involving these ligands are correctly determined with B3LYP despite the fact that the high spin state has four more unpaired electrons. Application of our previous spin-splitting DBLOC model to this independent test set of spin-crossover complexes is able to correctly reverse the B3LYP ordering of spin state energetics in nearly every case except for a few cases where the energies shift in the correct direction but fall slightly short by an amount within the inherent uncertainty in the parameter values, which we estimate to be at around 100−200 mV.

Our principal objective in this paper in using the DBLOC model is to determine the ground state spin configurations for reactants and products in the redox reactions that we are modeling. It is necessary to utilize the correct spin states in the reaction if a calculated redox potential is to be appropriately compared with experimental results. Below, we discuss various types of complexes in some detail and indicate which cases required DBLOC corrections to produce what we believe to be the correct spin states, and for which cases DBLOC substantially improves the energy gap between spin states but misses the correct ordering by a few kilocalories per mole. Overall, the success of DBLOC in improving our spin state assignments is quite substantial. It would in fact be possible to utilize the current data set specifically as a test set for the DBLOC spin-splitting model, quantitatively comparing theory and experimental results, keeping track of statistics, etc. We have not done this in the present paper because a significant amount of additional work would be required for a clean presentation, including careful analysis of the experimental data, identifying the spin states, elimination of test cases where the experimental data was problematic, and other problems which we have discussed in our previous publication in this area. The analysis performed here is sufficient to enable an evaluation of the DBLOC performance for redox processes. In future work, we will consider the spin-splitting data in more detail and perform a much more extensive analysis as outlined above. For the present, the results demonstrate that our redox analysis is in general highly consistent with the spin-splitting model, a point reinforced by thermodynamic cycle calculations which enable an explicit comparison of the spin-splitting and redox parameters for the same process, discussed below.

The well-known series of hexacyano complexes fills t_{2g} before e_g due to the large Δ_o for cyanide, according to the spectrochemical series, and B3LYP/LACV3P predicts the correct ground state multiplicity in each case.

Metallocenes in our database include complexes in which the metal center is sandwiched by two cpstar ($((C_5(CH_3)_5)^{-1}$) ligands. B3LYP/LACV3P predicts the correct ground state multiplicities in comparison to EPR measurements[81] in all but three cases, namely, $[Cr(II)(cpstar)_2]$, $[Mn(III)(cpstar)_2]^{+1}$, and $[Co(II)(cpstar)_2]$, for which the correct ground state is within a maximum of around 100−200 mV or 2.3−4.6 kcal/mol. In comparison to low temperature measurements,[81] B3LYP/LACV3P incorrectly predicts the $t_{2g}^1 t_{2g}^1 t_{2g}^1 e_g^1 e_g^0$ configuration of $[Cr(II)(cpstar)_2]$ to be the ground state, with the $t_{2g}^2 t_{2g}^1 t_{2g}^1 e_g^0 e_g^0$ configuration 200 mV higher in energy. Applying the DBLOC spin-splitting correction of *p-2ss-6exmss* (see Table 6 for a summary of the DBLOC spin-splitting parameters) or −215 mV correctly reorders the states for the $[Cr(II)(cpstar)_2]$ complex, making the $t_{2g}^2 t_{2g}^1 t_{2g}^1 e_g^0 e_g^0$ configuration the ground state configuration and putting the $t_{2g}^1 t_{2g}^1 t_{2g}^1 e_g^1 e_g^0$ configuration 15 mV higher in energy, a final result that is consistent with the small energy gaps needed for spin-crossover complexes. The LOC model applies similarly to the $[Mn(III)(cpstar)_2]^{+1}$ complex. B3LYP/LACV3P predicts a ground state configuration of $t_{2g}^2 t_{2g}^2 t_{2g}^1 e_g^1 e_g^1$ for the $[Co(II)(cpstar)_2]$ complex, which is in contrast to the low temperature experimental result and has the $t_{2g}^2 t_{2g}^2 t_{2g}^2 e_g^1 e_g^0$ configuration 100 mV higher in energy. Applying the *p-ss-6exmss* or −260 mV correction provides the correct ground state configuration of $t_{2g}^2 t_{2g}^2 t_{2g}^2 e_g^1 e_g^0$ with the $t_{2g}^2 t_{2g}^2 t_{2g}^1 e_g^1 e_g^1$ configuration 160 mV higher in energy. The *exmss* spin-splitting parameter is used in determining these corrections because experimental and calculated results suggest that the cpstar ligand lies to the middle-right of the spectrochemical series somewhere to the right of amine and to the left of ligands with aromatic nitrogens like phen, bpy, etc. Complexes like $[Cr(II)(phen)_3]^{+2}$ and $[Cr(II)(en)_3]^{+2}$ are low- and high-spin, respectively, while a complex, like $[Cr(II)(tpen)]^{+2}$, that mixes these two types of ligands is a spin-crossover complex like

$[Cr(II)(cpstar)_2]$, meaning that the cpstar ligand has an effect on the metal that is much like an average of effects due to ligands with amine and aromatic nitrogen coordinations, which respectively lie to the left and right of the cpstar ligand in the spectrochemical series.

As seen with both B3LYP and B3LYP with the DBLOC corrections, many of the metallocenes in our database were found to be spin-crossover complexes, which is in agreement with experimental results[82] as well as with the behavior observed in other complexes that have metals with relatively low oxidation states bound to ligands that are relatively far to the right of the spectrochemical series, for example, the $[Fe(II)(terpy)_2]^{+2}$ complex. All reduced complexes of this series are spin-crossover complexes, with the exception of the manganocene complex, where the high spin d^5 configuration provides extra stability. The Ni(II) metallocene has a fully filled t_{2g} manifold and two unpaired electrons in the e_g orbitals, and so spin-crossover in the current context does not apply. For the oxidized complexes, we hypothesize that the reason why the Mn(III) complex exhibits a spin-crossover while a complex like Fe(III) for example does not is due to the difference in effective nuclear charge on the two metal centers, which is known from basic inorganic chemistry to increase across the d-block of the periodic table as a result of decreased electron−electron repulsion and thus decreased atomic radii. This in turn provides a slight increase in the size of Δ_o, which is apparently enough to force borderline cases to become predominantly low spin.

In agreement with experimental results,[8,27] B3LYP/LACV3P predicts three of the tacn complexes, those involving Mn(III), Fe(II), and Co(II), to be spin-crossover complexes. Other complexes with +3 oxidation states do not exhibit spin-crossover due to the increase in effective nuclear charge. B3LYP/LACV3P predicts the correct ground state multiplicities in every case except $[Co(II)(tacn)_2]^{+2}$, where it predicts that the high spin complex is about 200 mV more stable than the low spin complex. As previously discussed for the metallocenes, applying the DBLOC spin-splitting correction of *p-ss-6exmss* or −260 mV to the $[Co(II)(tacn)_2]^{+2}$ complex provides the correct low spin ground state with the high spin state 160 mV higher in energy. This is because the cpstar and tacn ligands have similar positions in the spectrochemical series. For the complex $[Mn(III)(tacn)_2]^{+3}$, B3LYP/LACV3P predicts the correct low spin triplet ground state with the high spin quintet only 30 mV higher in energy. Applying DBLOC gives a correction of 215 mV, which is the same as the correction applied to the quintet to triplet transition for the $[Mn(III)(cpstar)_2]^{+1}$ metallocene except with opposite sign due to reversal of the physical process. This correction simply increases the triplet to quintet gap to 245 mV, which is still well within the acceptable range for spin-crossover.

The rationale for the electronic structures of the complexes in the tpen, tp (tris-pyrazolylborate), and terpy series follows similarly as for the tacn series except that now $[Cr(II)(tpen)]^{+2}$ and $[Cr(II)(tp)]$ also exhibit spin-crossover behavior due to the addition of aromatic nitrogens and a subsequent increase in Δ_o. B3LYP/LACV3P predicts the correct ground state multiplicities in nearly every case except for a few in which it slightly reverses the ordering of the states. In every one of those cases, DBLOC correctly decreases the energies of the appropriate states and makes them the ground states, with the exception of $[Co(II)(tpen)]^{+2}$ and $[Co(II)(tp)_2]$, where the DBLOC correction falls slightly short, within an amount less than 50 mV. The spin-crossover nature of $[Cr(II)(tp)_2]$ is questioned because tp is a ligand with exclusively coordinating aromatic nitrogens, yet the complex $[Cr(II)(phen)_3]^{+2}$, which also coordinates through six aromatic nitrogens, is low spin. Nevertheless, the B3LYP/LACV3P spin gaps for $[Cr(II)(tp)_2]$ and $[Cr(II)(phen)_3]^{+2}$ are about 0.1 V (2.5 kcal/mol) and 0.6 V (13.5 kcal/mol), respectively, and so it is hypothesized that there are rather significant differences between the two ligands in their electron donating character. In fact, phen, bpy, py26diox, and py2ox ligands all lie just outside the range necessary for spin-crossover. It is well-known[83,84] that $[Fe(II)(phen)_3]^{+2}$ becomes a spin-crossover complex when phen is substituted by two isothiocyanate ligands which decrease Δ_o, and similarly the $[Cr(III)(en)_2(ncs)_2]^{+1}/[Cr(II)(en)_2(ncs)_2]$ couple is found to be high spin due to small Δ_o.

Complexes that coordinate through oxygen atoms involve ligands that lie to the left of the spectrochemical series, and so the complexes tend to fill high spin. One exception is for complexes involving Co(III), which fully fill the t_{2g} manifold due to the increased effective nuclear charge. B3LYP/LACV3P predicts the correct ground state multiplicity in every case except $[Cr(II)(acac)_3]^{-1}$. In this case, B3LYP/LACV3P predicts a ground state triplet with a configuration of $t_{2g}^2 t_{2g}^1 t_{2g}^1 e_g^0 e_g^0$ and which is 160 mV below what is thought to be the correct low temperature ground state configuration of $t_{2g}^1 t_{2g}^1 t_{2g}^1 e_g^1 e_g^0$. Application of DBLOC provides a correction of *-p+6ss+6exlss* or −220 mV, which correctly reverses the ordering of the states. As discussed in our previous spin-splitting article,[27] it may be necessary to account for parallel spin−spin corrections between t_{2g} and e_g for complexes which have small Δ_o, for example, metal centers in low oxidation states and weakly interacting ligands like acac.

Ligands cl4bdt, mnt, and pdt coordinate through six anionic sulfurs and lie to the left of the spectrochemical series, causing their complexes to fill high spin. The $[Fe(IV)(cl4bdt)_3]^{-2}$ complex fills high spin despite the rather large positive oxidation state on iron, while the complex $[Ni(III)(s2cnet2)_3]$ fills low spin due to ligand resonance structures involving three anionic sulfurs and three thioketone sulfurs. B3LYP/LACV3P predicts the correct ground state multiplicities in every case, except for the $[Fe(IV)(cl4bdt)_3]^{-2}$ and $[Fe(III)(cl4bdt)_3]^{-3}$ complexes, where it predicts a ground state triplet for the oxidized complex and a ground state quartet for the reduced complex. Application of DBLOC to these cases does decrease the energy of the states, which are supposed to be the ground states, but however falls slightly short by an amount that is within the acceptable level of uncertainty in this work.

Complexes with both nitrogen and oxygen coordination, through ligands like hbed, edta, cdta, mida, ptda, h2o4phen, gly, h2o2phen2, etc., all tend to fill high spin for the reduced forms due to small Δ_o, and B3LYP/LACV3P agrees with this conclusion in every case. For the oxidized complexes, the anionic oxygen field is far enough to the left of the spectrochemical series that most of the complexes fill high spin. Other heteroleptic complexes can be understood by combining the principles outlined in the paragraphs above.

3.2. Ligand Additivity. To develop the LOC model for redox potentials, it is also necessary to understand how the principle of ligand additivity applies to the experimental and calculated potentials in our database. Table 3 includes a summary of the experimental and B3LYP redox potentials for three systematic series of complexes. The convention used in this work is that all redox potentials are reported as standard reduction potentials referenced to NHE and are labeled by the oxidized form of the corresponding redox couple. Both experimental results and

Table 3. Summary of the Redox Potentials of Three Different Series of Transition Metal Complexes from the Redox Database[a]

complex	coord.	exptl.	B3LYP	exptl. − B3LYP	*exptl.	*B3LYP	*exptl. − *B3LYP
$[Fe(III)(cn)_6]^{-3}$	c6	0.36	−0.33	0.69	0.36	−0.33	0.69
$[Fe(III)(bpy)(cn)_4]^{-1}$	c4n2	0.54	−0.15	0.69	0.61	0.01	0.61
$[Fe(III)(bpy)_2(cn)_2]^{+1}$	c2n4	0.78	0.20	0.58	0.87	0.34	0.52
$[Fe(III)(bpy)_3]^{+3}$	n6	1.12	0.68	0.44	1.12	0.68	0.44
$[Co(III)(ox)_3]^{-3}$	o6	0.57	0.05	0.52	0.57	0.05	0.52
$[Co(III)(ox)_2(h2o)_2]^{-1}$	o6	0.78	0.43	0.35	1.00	0.73	0.27
$[Co(III)(h2o)_6]^{+3}$	o6	1.86	2.10	−0.24	1.86	2.10	−0.24
$[Co(III)(phen)_3]^{+3}$	n6	0.33	0.00	0.33	0.33	0.00	0.33
$[Co(III)(h2o)_2(phen)_2]^{+3}$	n4o2	0.68	0.86	−0.18	0.84	0.70	0.14
$[Co(III)(h2o)_4(phen)]^{+3}$	n2o4	0.84	1.52	−0.68	1.35	1.40	−0.05
$[Co(III)(h2o)_6]^{+3}$	o6	1.86	2.10	−0.24	1.86	2.10	−0.24

[a]The asterisked columns correspond to redox potentials of heteroleptic complexes which are estimated from linear combinations of homoleptic complexes and are used to demonstrate the principle of ligand additivity. All potentials are reported in units of volts.

B3LYP show clear patterns in the redox potentials as one transforms $[Fe(III)(cn)_6]^{-3}$ into $[Fe(III)(bpy)_3]^{+3}$ or when either $[Co(III)(ox)_3]^{-3}$ or $[Co(III)(phen)_3]^{+3}$ is transformed into $[Co(III)(h2o)_6]^{+3}$. The B3LYP errors are largest for cases where the complexes are dominated by cyano ligands and smaller for complexes that are dominated by ligands that coordinate through aromatic nitrogens or, up to the uncertainty of experimental and calculated results, anionic oxygens like oxalate. Using the ligand additivity model, we will verify that the large error of −0.68 V for the $[Co(III)(h2o)_4(phen)]^{+3}$ couple is due to error in the reported experimental potential. Note that the B3LYP errors for $[Fe(III)(bpy)_3]^{+3}$ and $[Co(III)(phen)_3]^{+3}$ differ by only 0.11 V, which suggests that the error does not really depend on the metal center. As water ligands are added to the cobalt couples, the B3LYP errors cross through zero and become small and negative.

Using these three series of complexes, it is possible to test the principle of ligand additivity by simply representing each heteroleptic complex in terms of linear combinations of the corresponding homoleptic complexes as in eq 1. These estimates are given in the columns marked with an asterisk and are in agreement with the true experimental and/or calculated results in all cases except $[Co(III)(h2o)_4(phen)]^{+3}$, where there is a large difference of 0.51 V between the reported experimental value (0.84 V) and the value predicted by the simple ligand additivity model (1.35 V). Given other successes of the ligand additivity model, within Tables 3, 4, and 5 of this article as well as in previous work,[10−17,20−23] this large difference of 0.51 V suggests that the experimental value of 0.84 V reported for $[Co(III)(h2o)_4(phen)]^{+3}$ in ref 45 is incorrect. The value of this potential is not clear from ref 85, which is cited in ref 45. We believe that the correct value for the $[Co(III)(h2o)_4(phen)]^{+3}$ potential is closer to 1.35 V on the basis of the potentials for $[Co(III)(phen)_3]^{+3}$, as well as its bpy and terpy analogues, and $[Co(III)(h2o)_6]^{+3}$, which have been consistently measured to be about 0.33 and 1.86 V, respectively, in a number of different experiments.[45,72,73,86,87] Therefore, the experimental redox potential for this complex has been taken as 1.35 V instead of 0.84 V in the remainder of this article.

3.3. Redox Potentials. *3.3.1. Exact Nonlocal Exchange.* Systematic studies of the B3LYP redox errors like that presented in Table 3 were performed on all 95 complexes in our database, and the results are summarized in Tables 4 and 5. Redox couples are organized by coordinating atoms with homoleptic complexes first and heteroleptic complexes second and are marked by the column l.f.d. that indicates the electronic structure of the final reduced orbital. It is immediately obvious in Tables 4 and 5 that B3LYP incorrectly determines the redox potentials relative to experimental results and that the magnitude and sign of the errors depends on the coordinating ligands. As previously discussed in the Introduction, this is a result of incorrect B3LYP energetics for the d manifold, i.e., HOMO/LUMO t_{2g}/e_g orbitals. However, for a series of complexes like $[Cr(III)(phen)_3]^{+3}$, $[Fe(III)(phen)_3]^{+3}$, and $[Co(III)(phen)_3]^{+3}$, B3LYP systematically determines that the d manifold is on average 0.42 ± 0.10 V less than experimental results. Results like this are quite systematic over our database of 95 complexes, with the exception of Ni(III/II) redox couples, which have their own systematic error to be discussed below, and so we conclude that to first order the B3LYP errors with respect to experimental results generally shows only small dependence on metal center.

Ni(III/II) redox couples present an exception to this rule because their B3LYP errors with respect to experimental results, regardless of the ligand field, are systematically about 300−400 mV more negative than the average error over a given series of complexes, for example, as in $[Ni(III)(cpstar)_2]^{+1}$, $[Ni(III)(tacn)_2]^{+3}$, $[Ni(III)(tpen)]^{+3}$, and $[Ni(III)(tp)_2]^{+1}$ complexes. Every redox couple in the cpstar, tacn, tpen, and tp series, with the exception of the Ni couples as well as the $[Cr(III)(tacn)_2]^{+3}$ couple, which is a borderline case, involves spin-crossover for either the oxidized or reduced forms as well as only partially filled t_{2g} manifolds. Therefore, the DBLOC redox parameters that are fit to these couples additionally include in an average way formally nonzero multireference effects that are less prevalent in the Ni(III/II) redox potentials. For the Ni(III/II) redox couples, both oxidized and reduced forms have a fully filled t_{2g} manifold with only a small number of ways to arrange the remaining electrons in the e_g orbitals. For the Ni redox couples, spin-crossover in the current context does not apply, and so the d^7 $t_{2g}^2t_{2g}^2t_{2g}^2e_g^1e_g^0$ and d^8 $t_{2g}^2t_{2g}^2t_{2g}^2e_g^1e_g^1$ configurations are strong leading order determinants which are well represented by the simplified ligand field diagrams presented in Table 2. This is in contrast to the ligand field diagrams for the cpstar, tacn, tpen, and tp spin-crossover complexes, which are slightly more complicated due to a formally nonzero contribution from states with differing spin multiplicities as well as multireference aspects of the only partially filled t_{2g} manifold, and so these determinants are not as strongly leading order as those for the Ni(III/II) redox couples. The resulting spin contamination seen in these cases is very small compared to other sources of spin contamination seen in other types of calculations on transition metal complexes, for example, as in section 3.3.4 of the Results and Discussion section. We hypothesize that the differences in strength of leading order

dx.doi.org/10.1021/ct2006693 | J. Chem. TheoryComput. 2012, 8, 442−459

Table 4. Summary of Experimental, B3LYP, and DBLOC Redox Potentials for All Transition Metal Complexes in the Redox Database[a]

complex	solvent	coord.	l.f.d.	exptl.	exptl.-B3LYP	p	s	exlss	exmss	exrss	relss	remss	rerss	dif f	ra d	N^{-1}	Ni	DBLOC corr.	exptl. − DBLOC
$[Cr(III)(cn)_6]^{-3}$	water	c6	t_{2g}^2	−1.28	0.58	0	−2	0	0	0	0	0	6	0	0	0	0	0.71	−0.03
$[Mn(III)(cn)_6]^{-3}$	water	c6	t_{2g}^2	−0.24	0.81	0	−1	0	0	0	0	0	6	0	0	0	0	0.71	0.15
$[Fe(III)(cn)_6]^{-3}$	water	c6	t_{2g}^2	0.36	0.69	0	0	0	0	0	0	0	6	0	0	0	0	0.71	−0.02
$[Co(III)(cn)_6]^{-3}$	water	c6	e_g^1	−1.80	0.46	0	0	0	0	0	0	0	6	0	0	0	0	0.71	−0.25
$[Cr(III)(cpstar)_2]^{+1}$	acetonitrile	c6	t_{2g}^2	−0.81	0.21	0	−2	0	0	0	0	6	0	0	0	0	0	0.47	−0.16
$[Mn(III)(cpstar)_2]^{+1}$	acetonitrile	c6	e_g^1	−0.32	−0.66	−1	3	0	6	0	0	0	0	6	0	0	0	−0.56	0.03
$[Fe(III)(cpstar)_2]^{+1}$	dichloromethane	c6	t_{2g}^2	0.13	0.28	0	0	0	0	0	0	6	0	0	0	0	0	0.47	−0.19
$[Co(III)(cpstar)_2]^{+1}$	acetonitrile	c6	e_g^1	−1.24	−0.61	0	0	0	0	0	0	0	0	6	0	0	0	−0.56	−0.05
$[Ni(III)(cpstar)_2]^{+1}$	dichloromethane	c6	e_g^1	−0.41	−0.88	0	1	0	0	0	0	0	0	6	0	0	1	−0.95	0.02
$[Cr(III)(tacn)_2]^{+3}$	water	n6	e_g^1	−1.14	0.22	0	0	0	0	0	0	6	0	0	0	0	0	0.47	−0.25
$[Mn(III)(tacn)_2]^{+3}$	water	n6	e_g^1	0.62	0.32	−1	3	6	0	0	0	6	0	0	0	0	0	0.47	−0.26
$[Fe(III)(tacn)_2]^{+3}$	water	n6	t_{2g}^2	0.13	0.26	0	0	0	0	0	0	6	0	0	0	0	0	0.47	−0.21
$[Co(III)(tacn)_2]^{+3}$	water	n6	e_g^1	−0.40	0.36	0	0	0	0	0	0	6	0	0	0	0	0	0.47	−0.11
$[Ni(III)(tacn)_2]^{+3}$	water	n6	e_g^1	0.95	0.03	0	1	0	0	0	0	6	0	0	0	0	1	0.08	−0.10
$[Cr(III)(en)_3]^{+3}$	water	n6	e_g^1	−1.03	0.45	0	0	0	0	0	0	6	0	0	0	0	0	0.47	−0.02
$[Co(III)(den)_2]^{+3}$	water	n6	e_g^1	−0.23	0.57	0	0	0	0	0	0	6	0	0	0	0	0	0.47	0.10
$[Cr(III)(tpen)]^{+3}$	acetonitrile	n6	t_{2g}^2	−0.71	0.36	0	−2	0	0	0	0	6	0	0	0	0	0	0.47	−0.01
$[Mn(III)(tpen)]^{+3}$	acetonitrile	n6	e_g^1	1.33	0.53	−1	3	2	4	0	0	6	0	0	0	0	0	0.47	0.11
$[Fe(III)(tpen)]^{+3}$	acetonitrile	n6	t_{2g}^2	1.01	0.43	0	0	0	0	0	0	6	0	0	0	0	0	0.47	−0.04
$[Co(III)(tpen)]^{+3}$	acetonitrile	n6	e_g^1	0.51	0.62	0	0	0	0	0	0	6	0	0	0	0	0	0.47	0.15
$[Ni(III)(tpen)]^{+3}$	acetonitrile	n6	e_g^1	1.81	0.19	0	1	0	0	0	0	6	0	0	0	0	1	0.08	0.06
$[Cr(III)(tp)_2]^{+1}$	dichloromethane	n6	t_{2g}^2	−1.33	0.29	0	−2	0	0	0	0	6	0	0	0	0	0	0.47	−0.08
$[Mn(III)(tp)_2]^{+1}$	dichloromethane	n6	e_g^1	0.46	0.64	−1	3	0	6	0	0	6	0	0	0	0	0	0.47	0.30
$[Fe(III)(tp)_2]^{+1}$	dichloromethane	n6	t_{2g}^2	0.13	0.22	0	0	0	0	0	0	6	0	0	0	0	0	0.47	−0.25
$[Co(III)(tp)_2]^{+1}$	dichloromethane	n6	e_g^1	−0.13	0.47	0	0	0	0	0	0	6	0	0	0	0	0	0.47	0.00
$[Ni(III)(tp)_2]^{+1}$	dichloromethane	n6	e_g^1	1.21	0.01	0	1	0	0	0	0	6	0	0	0	0	1	0.08	−0.12
$[Mn(III)(terpy)_2]^{+3}$	water	n6	e_g^1	1.28	0.52	−1	3	0	6	0	0	6	0	0	0	0	0	0.47	0.18
$[Fe(III)(terpy)_2]^{+3}$	water	n6	t_{2g}^2	1.12	0.35	0	0	0	0	0	0	6	0	0	0	0	0	0.47	−0.12
$[Co(III)(terpy)_2]^{+3}$	water	n6	e_g^1	0.31	0.25	0	0	0	0	0	0	6	0	0	0	0	0	0.47	−0.22
$[Cr(III)(phen)_3]^{+3}$	water	n6	t_{2g}^2	−0.02	0.52	0	−2	0	0	0	0	6	0	0	0	0	0	0.47	0.15
$[Fe(III)(phen)_3]^{+3}$	water	n6	t_{2g}^2	1.13	0.40	0	0	0	0	0	0	6	0	0	0	0	0	0.47	−0.07
$[Co(III)(phen)_3]^{+3}$	water	n6	e_g^1	0.33	0.33	0	0	0	0	0	0	6	0	0	0	0	0	0.47	−0.14
$[Cr(III)(bpy)_3]^{+3}$	water	n6	t_{2g}^2	0.01	0.54	0	−2	0	0	0	0	6	0	0	0	0	0	0.47	0.17
$[Fe(III)(bpy)_3]^{+3}$	water	n6	t_{2g}^2	1.12	0.44	0	0	0	0	0	0	6	0	0	0	0	0	0.47	−0.03
$[Co(III)(bpy)_3]^{+3}$	water	n6	e_g^1	0.31	0.38	0	0	0	0	0	0	6	0	0	0	0	0	0.47	−0.09
$[Fe(III)(py26diox)_2]^{-1}$	water	n6	t_{2g}^2	0.20	0.76	0	0	0	0	0	0	2	4	0	0	0	0	0.63	0.13
$[Fe(III)(py2ox)_3]$	water	n6	t_{2g}^2	0.35	0.82	0	0	0	0	0	0	3	3	0	0	0	0	0.59	0.23
$[Cr(III)(en)_2(ncs)_2]^{+1}$	water	n6	e_g^1	−0.90	0.63	0	0	0	0	0	0	4	0	0	0	2	0	0.63	0.00
$[Ti(IV)(nap)_3]^{-2}$	water	o6	t_{2g}^1	−1.12	0.65	0	0	0	0	0	0	6	0	0	0	0	0	0.47	0.18
$[Fe(III)(nap)_3]^{-3}$	water	o6	t_{2g}^2	−0.58	0.40	0	−2	0	0	0	0	6	0	0	0	0	0	0.47	0.03
$[Ti(IV)(cit)_3]^{-2}$	water	o6	t_{2g}^1	−0.31	0.60	0	0	0	0	0	0	6	0	0	0	0	0	0.47	0.13

dx.doi.org/10.1021/ct2006693 | J. Chem. Theory Comput. 2012, 8, 442–459

Table 4. continued

complex	solvent	coord.	l.f.d.	exptl.	exptl.-B3LYP	p	s	e x l s	e x m s	e x r s	e e l s	e e m s	r r e s	s f i d	a r d	N^{-1}	N i	DBLOC corr.	exptl. − DBLOC
$[Fe(III)(cit)_3]^{-3}$	water	o6	t_{2g}^2	−0.08	0.34	0	−2	0	0	0	0	6	0	0	0	0	0	0.47	−0.03
$[Fe(III)(ox)_3]^{-3}$	water	o6	t_{2g}^2	0.01	0.53	0	−2	0	0	0	0	6	0	0	0	0	0	0.47	0.16
$[Co(III)(ox)_3]^{-3}$	water	o6	e_g^1	0.57	0.52	−1	1	6	0	0	0	6	0	0	0	0	0	0.47	0.04
$[V(III)(acac)_3]$	acetonitrile	o6	t_{2g}^1	−1.18	0.16	0	2	0	0	0	3	3	0	0	0	0	0	0.11	−0.05
$[Cr(III)(acac)_3]$	acetonitrile	o6	e_g^1	−1.57	0.45	0	0	0	0	0	3	3	0	0	0	0	0	0.11	0.34
$[Mn(III)(acac)_3]$	acetonitrile	o6	e_g^1	0.15	0.41	0	1	0	0	0	3	3	0	0	0	0	0	0.11	0.25
$[Fe(III)(acac)_3]$	acetonitrile	o6	t_{2g}^2	−0.43	0.17	0	−2	0	0	0	3	3	0	0	0	0	0	0.11	0.16
$[Co(III)(acac)_3]$	acetonitrile	o6	e_g^1	−0.11	0.10	−1	1	6	0	0	3	3	0	0	0	0	0	0.11	−0.02
$[Cr(III)(h2o)_6]^{+3}$	water	o6	e_g^1	−0.58	−0.17	0	0	0	0	0	6	0	0	0	0	0	0	−0.24	0.07
$[Mn(III)(h2o)_6]^{+3}$	water	o6	e_g^1	1.50	−0.15	0	1	0	0	0	6	0	0	0	0	0	0	−0.24	0.04
$[Fe(III)(h2o)_6]^{+3}$	water	o6	t_{2g}^2	0.75	−0.26	0	−2	0	0	0	6	0	0	0	0	0	0	−0.24	0.08
$[Co(III)(h2o)_6]^{+3}$	water	o6	e_g^1	1.86	−0.24	−1	1	6	0	0	6	0	0	0	0	0	0	−0.24	−0.01
$[Co(III)(ox)_2(h2o)_2]^{-1}$	water	o6	e_g^1	0.78	0.35	−1	1	6	0	0	2	4	0	0	0	0	0	0.23	0.11

[a]Rows are organized by types of coordinating atoms, homoleptic complexes first and heteroleptic complexes second. The type of reduced orbital created is indicated in the l.f.d. column. Parameter weights are for parameters in the standard reduction potential framework as given in Table 6. All potentials are reported in units of volts.

determinants between the nickel and non-nickel couples results in the more negative than average error seen for the Ni(III/II) redox couples. Other Ni(III/II) redox couples like $[Ni(III)(s2cnet2)_3]$, $[Ni(III)(edta)]^{-1}$, and $[Ni(III)(pdtc)_2]^{-1}$ appear to behave similarly, and thus in our final redox DBLOC model, we will incorporate a parameter specific to Ni but that in principle could be applied to other relevant transition metal centers that have ligand field diagrams that are strongly dominated by one particular determinant, which corrects for this relative bias in the redox potentials.

While the dominant error in B3LYP redox potentials for transition metal complexes is in the energies of the HOMO/LUMO orbitals and has little to do, with the exception of the Ni(III/II) redox couples discussed above, with the identity of the metal center itself, other series, for example the tp series as compared to the phen series, while having similar average errors have a significantly larger standard deviation of 250 mV and a significantly larger than average error of 0.64 V for the $[Mn(III)(tp)_2]^{+1}$ redox couple. Some couples belonging to other series also have larger than average errors, for example, $[Mn(III)(terpy)_2]^{+3}$, $[Mn(III)(tpen)]^{+3}$, and other couples, including some of the Co(III/II) couples, to a lesser extent. It can be seen in the ligand field diagrams given in Table 2 that these couples all feature an increase of three in the number of unpaired electrons upon reduction, which is in contrast to the many other couples in the database for which this change is ±1. This suggests a second smaller systematic error contribution to the B3LYP redox potentials which results from B3LYP's overstabilization of the high spin reduced complexes that when added to the larger HOMO/LUMO error component results in larger than average errors for redox couples where the number of unpaired electrons substantially increases upon reduction. In some of the cases where the number of unpaired electrons increases by three, the presence of various sources of noise make it difficult to ascribe these larger than average errors to exact nonlocal exchange contributions. When combined with the fact that for the great majority of the redox couples considered in our database the number of unpaired electrons changes by ±1 upon reduction, where the effects due to exact nonlocal exchange tend to cancel between oxidized and reduced forms and thus to first order the B3LYP redox errors appear largely independent of metal center, we found that it was unnecessary to extend our proposed model to explicitly include these effects.

For cases where the number of unpaired electrons does change significantly, increasing the amount of exact nonlocal exchange in B3LYP decreases the error for complexes with a low spin to high spin redox potential. As an example, consider the redox couple for the $[Mn(III)(tp)_2]^{+1}$ complex, which from Table 2 can be seen to simultaneously involve a triplet to sextet spin-crossover transition worth three extra unpaired electrons in the reduced state. The typical 20% exact nonlocal exchange results in an error with respect to experimental results of 0.64 V, as shown in Table 4, while increasing the amount of exchange to 25% results in a smaller error of −0.10 V and decreasing the amount of exchange to 15% results in a larger error of 1.35 V. This concept also applies to our above discussion regarding the errors for the Ni(III/II) redox couples being more negative than the average error for a given ligand series. The Ni(III/II) doublet d^7 and triplet d^8 ligand field diagrams are strongly leading order determinants and thus retain their full doublet and triplet characteristics, and so the change in the number of unpaired electrons is one full electron, which causes the reduced state to be overstabilized by exact nonlocal exchange to a greater extent than other ligand field diagrams

dx.doi.org/10.1021/ct2006693 | J. Chem. TheoryComput. 2012, 8, 442−459

Table 5. Summary of Experimental, B3LYP, and DBLOC Redox Potentials (Cont.) for All Transition Metal Complexes in the Redox Database[a]

complex	solvent	coord.	l.f.d.	exptl.	exptl. − B3LYP	p	ss	exlss	exmss	exrss	rellss	relmss	relrss	difff	rad	N^{-1}	Ni	DBLOC corr.	exptl. − DBLOC
$[Ti(IV)(cl4bdt)_3]^{-2}$	dichloromethane	s6	t_{2g}^1	−0.80	−0.22	0	0	0	0	0	6	0	0	0	0	0	0	−0.24	0.02
$[V(IV)(cl4bdt)_3]^{-2}$	dichloromethane	s6	t_{2g}^1	−0.75	−0.23	0	1	0	0	0	6	0	0	0	0	0	0	−0.24	−0.04
$[Cr(IV)(cl4bdt)_3]^{-2}$	dichloromethane	s6	t_{2g}^1	−0.12	−0.10	0	2	0	0	0	6	0	0	0	0	0	0	−0.24	0.04
$[Mn(IV)(cl4bdt)_3]^{-2}$	dichloromethane	s6	e_g^1	−0.70	−0.55	0	0	0	0	0	6	0	0	0	0	0	0	−0.24	−0.31
$[Mn(III)(cl4bdt)_3]^{-3}$	dichloromethane	s6	e_g^1	−0.88	−0.13	0	1	0	0	0	6	0	0	0	0	0	0	−0.24	0.06
$[Fe(IV)(cl4bdt)_3]^{-2}$	dichloromethane	s6	e_g^1	−0.53	−0.20	0	1	0	0	0	6	0	0	0	0	0	0	−0.24	−0.01
$[Fe(III)(cl4bdt)_3]^{-3}$	dichloromethane	s6	t_{2g}^2	−1.27	−0.26	0	−2	0	0	0	6	0	0	0	0	0	0	−0.24	0.08
$[V(IV)(mnt)_3]^{-2}$	dichloromethane	s6	t_{2g}^1	−0.32	−0.20	0	1	0	0	0	6	0	0	0	0	0	0	−0.24	−0.01
$[V(III)(mnt)_3]^{-3}$	dichloromethane	s6	t_{2g}^1	−1.50	0.03	0	2	0	0	0	6	0	0	0	0	0	0	−0.24	0.17
$[V(V)(pdt)_3]^{+1}$	dichloromethane	s6	t_{2g}^1	1.28	−0.43	0	0	0	0	0	6	0	0	0	0	0	0	−0.24	−0.19
$[V(IV)(pdt)_3]^{-2}$	dichloromethane	s6	t_{2g}^1	−1.61	−0.27	0	1	0	0	0	6	0	0	0	0	0	0	−0.24	−0.08
$[Ni(III)(s2cnet2)_3]$	acetonitrile	s6	e_g^1	−0.08	−0.56	0	1	0	0	0	6	0	0	0	0	0	1	−0.62	0.01
[Ti(IV)(hbed)]	water	n2o4	t_{2g}^1	−0.64	0.42	0	0	0	0	0	0	6	0	0	0	0	0	0.47	−0.05
$[Fe(III)(hbed)]^{-1}$	water	n2o4	t_{2g}^2	−0.37	0.68	0	−2	0	0	0	0	6	0	0	0	0	0	0.47	0.31
[Ti(IV)(edta)]	water	n2o4	t_{2g}^1	0.02	0.23	0	0	0	0	0	0	6	0	0	0	0	0	0.47	−0.24
$[V(III)(edta)]^{-1}$	water	n2o4	t_{2g}^1	−1.04	0.23	0	2	0	0	0	0	6	0	0	0	0	0	0.47	−0.34
$[Cr(III)(edta)]^{-1}$	water	n2o4	e_g^1	−0.98	0.42	0	0	0	0	0	0	6	0	0	0	0	0	0.47	−0.05
$[Fe(III)(edta)]^{-1}$	water	n2o4	t_{2g}^2	0.12	0.48	0	−2	0	0	0	0	6	0	0	0	0	0	0.47	0.11
$[Co(III)(edta)]^{-1}$	water	n2o4	e_g^1	0.37	0.51	−1	1	6	0	0	0	6	0	0	0	0	0	0.47	0.03
$[Ni(III)(edta)]^{-1}$	water	n2o4	e_g^1	1.29	0.33	0	1	0	0	0	0	6	0	0	0	0	1	0.08	0.20
[Ti(IV)(cdta)]	water	n2o4	t_{2g}^1	−0.02	0.20	0	0	0	0	0	0	6	0	0	0	0	0	0.47	−0.27
$[Cr(III)(cdta)]^{-1}$	water	n2o4	e_g^1	−0.96	0.48	0	0	0	0	0	0	6	0	0	0	0	0	0.47	0.01
$[Fe(III)(cdta)]^{-1}$	water	n2o4	t_{2g}^2	0.04	0.43	0	−2	0	0	0	0	6	0	0	0	0	0	0.47	0.06
$[Co(III)(cdta)]^{-1}$	water	n2o4	e_g^1	0.35	0.59	−1	1	6	0	0	0	6	0	0	0	0	0	0.47	0.11
$[Cr(III)(mida)_2]^{-1}$	water	n2o4	e_g^1	−1.16	0.61	0	0	0	0	0	0	6	0	0	0	0	0	0.47	0.14
$[Co(III)(pdta)]^{-1}$	water	n2o4	e_g^1	0.36	0.60	−1	1	6	0	0	0	6	0	0	0	0	0	0.47	0.12
$[Co(III)(h2o)_4(phen)]^{+3}$	water	n2o4	e_g^1	1.35	−0.17	−1	1	4	2	0	4	2	0	0	0	0	0	0.00	−0.10
$[Co(III)(gly)_3]$	water	n3o3	e_g^1	0.20	0.60	−1	1	6	0	0	0	6	0	0	0	0	0	0.47	0.12
$[Co(III)(h2o)_2(phen)_2]^{+3}$	water	n4o2	e_g^1	0.68	−0.18	−1	1	2	4	0	2	4	0	0	0	0	0	0.23	−0.26
$[Fe(III)(bpy)_2(cn)_2]^{+1}$	water	c2n4	t_{2g}^2	0.78	0.58	0	0	0	0	0	0	4	2	0	0	0	0	0.55	0.03
$[Cr(III)(cyclam)(cn)_2]^{+1}$	water	c2n4	t_{2g}^2	−1.12	0.70	0	−2	0	0	0	0	4	2	0	0	0	0	0.55	0.25
$[Cr(III)(en)_2(cn)_2]^{+1}$	water	c2n4	t_{2g}^2	−1.22	0.55	0	−2	0	0	0	0	4	2	0	0	0	0	0.55	0.10
$[Fe(III)(bpy)(cn)_4]^{-1}$	water	c4n2	t_{2g}^2	0.54	0.69	0	0	0	0	0	0	2	4	0	0	0	0	0.63	0.06
$[Cr(0)(co)_5(pycn)]$	water	c5n1	e_g^1	−1.03	0.39	0	0	0	0	0	0	1	5	0	0	0	0	0.67	−0.28
$[Mn(III)(cn)_5(no)]^{-2}$	water	c5n1	t_{2g}^2	0.60	−0.43	0	−1	0	0	0	0	0	5	0	1	0	0	−0.27	−0.12
$[Fe(III)(cn)_5(no)]^{-2}$	water	c5n1	t_{2g}^2	−0.07	−0.15	0	0	0	0	0	0	0	5	0	1	0	0	−0.27	0.12
$[Ni(III)(pdtc)_2]^{-1}$	water	n2s4	e_g^1	0.16	−0.40	0	1	0	0	0	4	2	0	0	0	0	1	−0.39	−0.06
$[Mn(III)(cl)(l52)]^{+2}$	water	cl1n5	e_g^1	1.19	0.21	−1	3	3	3	0	1	5	0	0	0	0	0	0.35	−0.13

dx.doi.org/10.1021/ct2006693 | J. Chem. Theory Comput. 2012, 8, 442–459

Table 5. continued

complex	solvent	coord.	l.f.d.	exptl.	exptl. − B3LYP	p	ss	exlss	exmss	exrss	relss	remss	rerss	diff	rad	N^{-1}	Ni	DBLOC corr.	exptl. − DBLOC
$[Fe(III)(cl)(l52)]^{+2}$	water	cl1n5	t_{2g}^2	0.81	0.32	0	−2	0	0	0	1	5	0	0	0	0	0	0.35	0.07
$[Cr(III)(cl)(l15)]^{+2}$	water	cl1n5	e_g^1	−0.85	0.29	0	0	0	0	0	1	5	0	0	0	0	0	0.35	−0.06
$[Cr(III)(cyclam)(cl)_2]^{+1}$	water	cl2n4	e_g^1	−0.75	−0.03	0	0	0	0	0	2	4	0	0	0	0	0	0.23	−0.26

[a] Rows are organized by types of coordinating atoms, homoleptic complexes first and heteroleptic complexes second. The type of reduced orbital created is indicated in the l.f.d. column. Parameter weights are for parameters in the standard reduction potential framework as given in Table 6. All potentials are reported in units of volts.

Table 6. Collection of the New Seven DBLOC Parameters for Computing Standard Reduction Potentials versus NHE Plus the Original Five Spin-Splitting Parameters Which Have Been Converted from the Thermodynamic Framework, $\Delta G^o_{1/2}$, in kcal/mol to the Electrochemical Framework, $E^o_{1/2}$, in Volts by Multiplying by −0.04336 V/(kcal/mol) According to eq 2

symbol	description	value/V
p	create a doubly occupied orbital	−0.44
ss	create a singly occupied−singly occupied interaction	0.05
exlss	$t_{2g}\rightarrow e_g$ excitation (left spectrochemical series)	−0.08
exmss	$t_{2g}\rightarrow e_g$ excitation (middle spectrochemical series)	−0.12
exrss	$t_{2g}\rightarrow e_g$ excitation (right spectrochemical series)	−0.23
relss	$\infty \rightarrow t_{2g}$ reduction (left spectrochemical series)	−0.04
remss	$\infty\rightarrow t_{2g}$ reduction (middle spectrochemical series)	0.08
rerss	$\infty \rightarrow t_{2g}$ reduction (right spectrochemical series)	0.12
diff	diffuse character of reduced orbital	−0.09
rad	radical character of coordinating atoms	−0.86
N^{-1}	anionic nitrogen character of coordinating atoms	0.16
Ni	d^7/d^8 strong leading order determinants	−0.38

that lack strongly leading order determinants but that also feature an increase of one in the number of unpaired electrons.

Decreasing the amount of exact nonlocal exchange, as in B3LYP*, which reduces it from 20% to 15%,[84,88] increases the error for such low spin to high spin redox potentials but, however, can decrease the error for a high spin to low spin reduction. While there are zero complexes of this type in our database for which the change in the number of unpaired electrons decreases by three, we do have some examples where this number decreases by one; for example, consider the redox couple for the $[Fe(III)(cl4bdt3)_3]^{-3}$ complex shown in Table 2. For this couple, the typical 20% exact nonlocal exchange results in an error with respect to experimental results of −0.26 V, as in Table 5, while increasing the amount of exchange to 25% results in a larger error of −0.74 V and decreasing the amount of exchange to 15% results in a smaller error of 0.19 V. In the general case, changing the amount of exact nonlocal exchange is certainly insufficient to correct all of the redox potentials; as an example, consider the cyano series where $[Co(III)(cn)_6]^{-3}$ increases the number of unpaired electrons by one upon reduction, while $[Mn(III)(cn)_6]^{-3}$ decreases the number of unpaired electrons by one upon reduction, yet the error for the Mn complex is significantly larger than the error for the Co complex. Since the majority of the 95 complexes are III/II couples, the reduced states tend to be high spin, and thus increasing the amount of exact nonlocal exchange may help in a few instances but does not offer a general solution to the problem. In fact, based on our results, it appears that 20% exact nonlocal exchange is about the amount needed to obtain a relatively small error in the redox potentials averaged over potentials involving different types of changes in spin states.

3.3.2. Spectrochemical Series. The unique amounts by which a given ligand field shifts the energy of the metal's d manifold relative to the free metal center, give rise to the differences seen in experimental and/or B3LYP redox potentials for different complexes; however understanding how the B3LYP errors depend on ligands is a bit different. The first generation DBLOC model for redox potentials attempted to describe the error pattern using coordinating ligand atom types featuring different numbers of lone pairs, different anionic character, etc. For example, a certain correction was assigned to atoms with a single lone pair like a cyano carbon, aromatic nitrogen, amino nitrogen, etc., while a different

correction was assigned to atoms with two lone pairs like an etheric or doubly bonded oxygen, doubly bonded sulfur, etc. Anionic corrections were then assigned for nitrogen, oxygen, sulfur, chlorine, etc.

When this parameter set was investigated more closely along with the mixing behavior of metal and ligand orbitals, it was found that the B3LYP redox errors were correlated with the spectrochemical series, which provides an approximate correlation with metal−ligand bond strengths. From our previous work on a LOC scheme for transition metal complexes,[27] we showed that B3LYP makes a systematic error in Δ_o depending on the strength of the metal−ligand bond and thus on the position of the ligands in the spectrochemical series. It was found that B3LYP underestimates the size of Δ_o, overbinding e_g orbitals with respect to the t_{2g} orbitals, to a greater extent as one moves right in the spectrochemical series toward more strongly interacting ligands and vice versa for ligands that lie to the left of the spectrochemical series. On the basis of systematic studies performed on large and diverse databases of spin-splitting and redox data for transition metal complexes, we have found that B3LYP makes systematic errors in the strength of metal−ligand interactions which manifest themselves in two different physical ways, namely, in the total energies of the d orbitals, which are reflected in redox errors, and in the energies of the e_g orbitals relative to the t_{2g} orbitals, which are reflected in spin-splitting errors. These two types of B3LYP errors both correlate with the spectrochemical series where the former case can be understood by considering that the total d-orbital energies, the energy depth on a molecular orbital diagram, are representative of the strength of the metal−ligand interaction.

3.3.3. DBLOC Model. Tables 4 and 5 show that the DBLOC model for redox potentials amounts to an extra energy correction term that is built upon the existing five-parameter DBLOC model that was determined from our previous work on spin-splittings.[27] This provides a single functional form that can be applied to the B3LYP energies of reactants and products, where the reactants and products can differ in the arrangement of d-orbital electrons, as in a spin-splitting reaction, or additionally can differ in the number of electrons, as in a redox reaction. As previously mentioned, there is a second manifestation of spin-crossover, namely where the reduction induces a spin-crossover.[8] In these cases, the spin-splitting parameters will be used again to correct the spin-crossover components of the spin-crossover coupled redox reactions, as shown in Tables 4 and 5. With the exception of the parallel spin−spin correction, there are only a few complexes whose reduction also involves physical processes described by the previous spin-splitting parameters; for example, see the eighth and 15th rows of Table 2. Spin-splitting parameters are applied to these complexes; however, as shown in Tables 4 and 5, their combined contribution to this particular type of application is quite small, amounting to a maximum of −0.15 V. The *exrss* parameter is shown in Tables 4 and 5 for completeness; however, it was not needed for this redox database because the database does not contain any examples of complexes undergoing spin-splitting processes in which the complex binds ligands that are to the right of the spectrochemical series.

After application of the previous set of spin-splitting parameters, we apply the new set of seven redox parameters as in the following equation:

$$E_{\mathrm{corr}}^{\mathrm{DBLOC}} = \sum_{i=1}^{6} (relss\delta_{L_i0} + remss\delta_{L_i1} + rerss\delta_{L_i2} + rad\delta_{L_irad} + N^{-1}\delta_{L_iN^{-1}}) \quad (3)$$

to arrive at the total redox correction. In principle, this sum is multiplied by ${}^{k}n^{t_{2g}} + {}^{k}n^{e_g} - {}^{0}n^{t_{2g}} - {}^{0}n^{e_g}$, where the set of n parameters signifies the number of electrons in the t_{2g} or e_g manifolds for either oxidized (reactant or 0th state) or reduced (product or kth state) forms; however, for single-electron reduction reactions, as opposed to those involving multiple electrons which were not considered in this database, its value is one. The *diff* and *Ni* parameters have not been shown in the above equation. The set of L_i is discussed in our previous article[27] and contains integers assigned to coordinating atoms to describe their positions in the spectrochemical series (0 to the left, 1 to the middle, 2 to the right, *rad* for radical character, and N^{-1} for nitrogens with significant negative charge), for example, six integers for the six coordinating atoms in the case of an octahedral complex. The diffuse parameter is needed when an electron is added to a highly diffuse orbital, for example, as in the e_g orbitals of the metallocene complexes that tend to spill out into unoccupied space, resembling the orbitals of the free metal center because they lack a full coordination sphere. For the metallocenes, there is a very clear distinction between the reduction of a t_{2g}-like orbital and an e_g-like orbital, giving further support for the two-level system also seen in ref 80. The radical parameter is meant to describe ligands that may retain some doublet character, for example, $NO^{\bullet}$ in the $[Mn(III)(CN)_5NO]^{-2}$ and $[Fe(III)(CN)_5NO]^{-2}$ complexes. The anionic nitrogen parameter is used in complexes which coordinate a nitrogen with significant negative charge, as in the $[Cr(III)(en)_2(ncs)_2]^{+1}$ complex. The *Ni* parameter is used in cases where the simplified ligand field diagrams, shown in Table 2, are themselves strongly leading order determinants, for example, as in redox couples with fully filled t_{2g} manifolds without spin-crossovers. The remaining *relss*, *remss*, and *rerss* parameters correlate with the spectrochemical series and describe B3LYP's error in HOMO/LUMO energetics. It is interesting that the binning of ligands in the spectrochemical series as determined from fitting B3LYP redox errors is nearly equivalent to the binning determined from our previous fitting of B3LYP spin-splitting errors. All parameters are given in Table 6 along with their description.

The final DBLOC model brings the mean unsigned error (MUE) of B3LYP with respect to experimental results from 0.40 ± 0.20 V (0.88 V max error) to 0.12 ± 0.09 V (0.34 V max error), and B3LYP is outperformed by DBLOC in nearly every case except for $[V(III)(mnt)_3]^{-3}$ and $[Cr(III)(cyclam)(cl)_2]^{+1}$, where the DBLOC errors are slightly larger, by 0.14 and 0.23 V, respectively, than B3LYP. For the complexes $[Fe(III)(py26diox)_2]^{-1}$ and $[Fe(III)(py2ox)_3]$, which coordinate through six aromatic nitrogens, four and three of those aromatic nitrogens respectively are more strongly interacting because they are directly bound to anionic oxygen. Those coordinating atoms are grouped with the most strongly interacting ligands. Returning to the $[Co(III)(en)_3]^{+3}$ complex in Table 1, which was originally removed from our database because its experimental value was recorded as 0.18 V rather than −0.18 V, and using it as a test case for applying the DBLOC method shows that its B3LYP redox potential of −0.53 V is corrected to be −0.05 V, which reduces the error with respect to experimental results from 0.35 V to −0.13 V. Experimental and calculated total standard reduction half potentials for all 95 complexes in DBLOC are summarized in Figure 1, and all DBLOC parameters (five old and seven new) used in Tables 4 and 5 and Figure 1 are given in Table 6 in units of volts. In Table 6, all parameters are reported in the electrochemical framework (as in the difference between thermodynamic, $\Delta G^{o}_{1/2}$, and electrochemical, $E^{o}_{1/2}$, measurements as in eq 2) and

dx.doi.org/10.1021/ct2006693 | J. Chem. TheoryComput. 2012, 8, 442−459

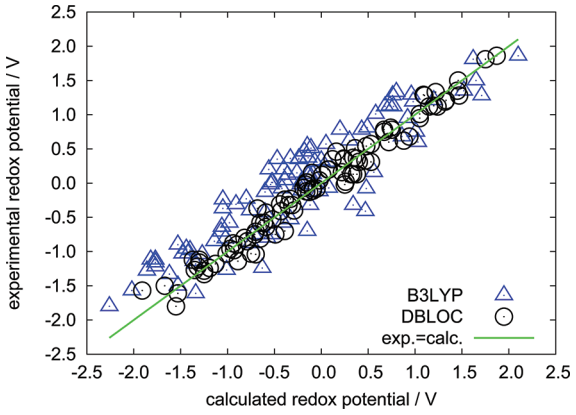

Figure 1. Experimental redox potentials versus calculated redox potentials for B3LYP and DBLOC over the 95 redox couples in the redox database.

can be used directly to compute standard reduction potentials versus NHE.

3.3.4. Connecting Spin-Splitting and Redox Models. Comparing the ligand field diagrams presented in Table 2 with those from our previous work[27] reveals that there should be a connection between the new redox parameters and the previously defined pairing parameter. While both parameters describe the unpairing of a doubly occupied d orbital, each marks a different physical process, i.e., removal of the electron to infinity in the case of a redox reaction that changes the total number of electrons or removal of the electron to another d orbital in the case of a spin-splitting that keeps the total number of electrons constant. In order to show the connection between the two parameters, we consider the simple case of electronic transitions in the t_{2g} manifold of $[Cr(III)(phen)_3]^{+3}$ which are shown in the thermodynamic cycle presented in Figure 2. In this

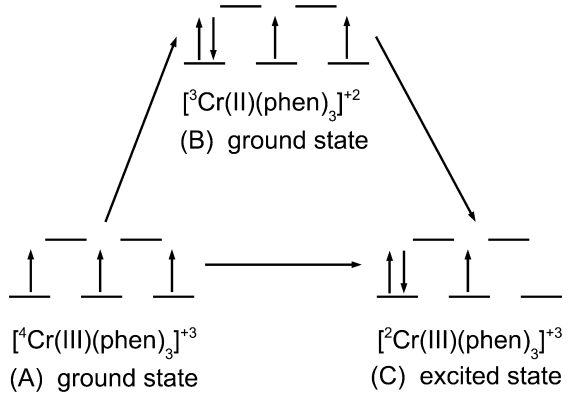

Figure 2. Thermodynamic cycle of ground state oxidized, ground state reduced, and excited state oxidized $[Cr(III)(phen)_3]^{+3}$ used to connect the spin-crossover and redox DBLOC parameters.

figure, A represents the $[Cr(III)(phen)_3]^{+3}$ quartet ground state, B represents the $[Cr(II)(phen)_3]^{+2}$ triplet ground state obtained from A by single-electron reduction, and C represents a $[Cr(III)(phen)_3]^{+3}$ doublet excited state obtained from A via spin-crossover or obtained from B via ionization. The B3LYP correction for the A to C transition is known from our previous work on spin-splittings to be *p-3ss* (13.20 kcal/mol thermodynamically or −0.57 V electrochemically). The B3LYP correction for the A to B transition is known from our current work on redox potentials to be *6remss-2ss* (0.38 V electrochemically) because the phen ligand is to the middle-right of the spectrochemical series. The C to B transition is a special case because it is a redox reaction that involves an excited state.

The complex $[Cr(III)(phen)_3]^{+3}$ was specifically chosen because the reduction of its doublet excited state has been measured in a number of different experiments[75,89−91] performed in both acetonitrile and water solvent at roughly the same temperature. Three articles[89−91] report this redox potential at around 1.42−1.47 V versus NHE, while another more recent article[75] reports the potential at around 1.05 V versus Fc^+/Fc. As discussed in the literature,[43] caution should be used when comparing redox potentials measured in acetonitrile with respect to different reference potentials; for example, that reference reports the potential of Fc^+/Fc at 0.63 V relative to NHE while another reference[75] reports a value of 0.56 V. Yet a value closer to 0.40 V would bring the $[Cr(III)(phen)_3]^{+3}$ potential reported at 1.05 V in ref 75 closer to the 1.42−1.47 V range which has been consistently measured in the past.[89−91] For this reason, we consider two values, 1.68 and 1.47 V, for the $[Cr(III)(phen)_3]^{+3}$ excited state doublet redox potential relative to NHE.

Similar to $[Cr(III)(en)_3]^{+3}$ and other complexes, including those with coordinating atoms other than nitrogen, from our previous article in which we investigated $t_{2g} \rightarrow t_{2g}$ spin-splitting energies,[27] B3LYP/LACV3P predicts two kinds of states in the excited state doublet manifold of $[Cr(III)(phen)_3]^{+3}$. One state is a high-energy pure spin-restricted doublet state, while the other is a low-energy spin-contaminated doublet state. The redox reaction to produce the ground state triplet $[Cr(II)(phen)_3]^{+2}$ complex (see B in Figure 2) by reducing the excited state doublet $[Cr(III)(phen)_3]^{+3}$ complex (see C in Figure 2) has a potential of 1.62 V if the doublet $[Cr(III)(phen)_3]^{+3}$ complex exists in the pure spin state and a potential of 0.56 V if the doublet is in the contaminated spin state. For a number of reasons explained in our previous paper,[27] the lower-energy spin-contaminated doublet state, which has a redox potential of 0.56 V, is in fact the correct state to compare with the experimental results.[75] In these experiments, the redox potential of the long-lived excited state doublet $[Cr(III)(phen)_3]^{+3}$ has been measured following the spin-forbidden UV−vis absorption of the ground state quartet $[Cr(III)(phen)_3]^{+3}$ complex (see A in Figure 2). Spin-forbidden transitions have zero dipole oscillator strength, and so the transition to the doublet state from the quartet state borrows intensity from neighboring spin-allowed quartet to quartet transitions, resulting in an excited state doublet that is contaminated with the quartet wave function. Other reasons confirming that our mapping of the B3LYP/LACV3P excited state energies to experimental results are correct are outlined in our previous paper on spin-splitting energies.[27]

Using the experimental reduction potentials of either 1.68 or 1.47 V and the B3LYP/LACV3P reduction potential of 0.56 V gives a calculated error (exptl. − calcd.) of either −1.12 V or −0.91 V for the B to C oxidation potential, where the sign of the error has been reversed in correspondence with ionization (oxidation) instead of attachment (reduction). This error represents an estimate of a new type of DBLOC parameter, which is much like the *remss* parameter except that it is for the reduction of the excited state doublet $[Cr(III)(phen)_3]^{+3}$ complex instead of the ground state quartet $[Cr(III)(phen)_3]^{+3}$ complex. As we go from B to C, there is an additional −1 (0.05) V due to the loss of a parallel spin−spin interaction giving −1.17 V or −0.96 V for the total B to C transition. The A to B to C transition can be computed to be −0.79 V or −0.58 V,

dx.doi.org/10.1021/ct2006693 | J. Chem. TheoryComput. 2012, 8, 442−459

which is in agreement with the −0.57 V result for the A to C transition. Thus, within the acceptable level of uncertainty in this work, experimental and calculated results have been connected between two different kinds of physical processes, electrochemical redox processes in solution and spectroscopic spin-forbidden processes in solution.

Another connection between the spin-splitting and redox LOC models is that they both correlate with the spectrochemical series. In Figure 3, we plot those DBLOC parameters that

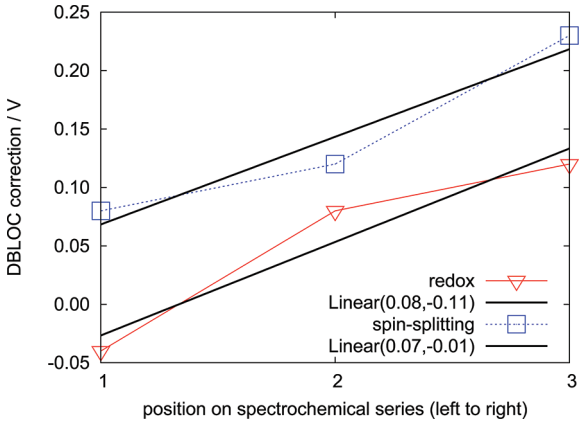

Figure 3. DBLOC parameters from the redox and spin-splitting models which correlate with the spectrochemical series. To the left are the weakly interacting ligands, and to the right are the strongly interacting ligands. Linear fits show that the slopes of the two sets of parameters are nearly identical, while the redox parameters can be derived from the spin-splitting parameters by a vertical shift of 100 mV. In this figure, all parameters are represented in the original spin-splitting thermodynamic framework, $\Delta G^{o}_{1/2}$, as in eq 2.

correlate with the spectrochemical series, including from Table 6 those used to correct spin-splitting energies, i.e., the $t_{2g} \rightarrow e_g$ parameters from our previous paper,[27] as well as those used to correct redox energies, i.e., the $t_{2g} \rightarrow \infty$ parameters from the current work. In that figure, the parameters are represented in the original thermodynamic framework in units of volts. It can be seen that for strongly interacting ligands which lie to the right of the spectrochemical series, the corrections are large and positive, indicating that B3LYP both (1) overbinds the t_{2g} and e_g orbitals by about 0.12 V per coordinating atom and (2) underestimates the t_{2g} to e_g energy gap, by additional overbinding of the e_g orbitals with respect to the t_{2g} orbitals, by about 0.23 V per coordinating atom. For weakly interacting ligands which lie to left of the spectrochemical series, we see that the corrections become smaller in magnitude and become negative for the redox potentials, indicating that B3LYP is underbinding the t_{2g} and e_g orbitals by about −0.04 V per coordinating atom.

As pointed out in the previous work,[27] the binning of the ligands in the spectrochemical series should be replaced by a continuous description with regard to some parameter, for example, explicit metal−ligand interaction energies; however, it is challenging to find sufficient ligand instances to make fitting such a detailed function possible. Due to various noise sources in both experimental results and computation, this is a challenging task, which we have not attempted to date. The parameters for both the spin-splitting and redox databases are both linearly correlated with respect to the spectrochemical series, having nearly the same slope and only a small difference of 100 mV in the y intercept, which is well within the acceptable level of uncertainty in this work and demonstrates that the two parameters sets are fully compatible, as is required by the physical picture we have postulated in both our previous spin-splitting article[27] and the present article.

4. APPLICATION TO CYTOCHROME P450

Recently, the long sought principal intermediate compound I responsible for C−H bond activation in cytochrome $P450_{119}$ was kinetically characterized by Rittle and Green[3] by preparing it in high yield via a reaction of ferric CYP119 (*Sulfolobus acidocaldarius*) with *m*-chloroperbenzoic acid. Using EPR, the electronic structure of the key intermediate was determined to be a doublet, i.e., a triplet Fe(IV)═O moiety that is antiferromagnetically coupled to a single electron delocalized over the porphyrin and thiolate ligands. A lower bound for the first order rate constant of $k \geq 210\ s^{-1}$ was determined for the hydroxylation of lauric acid substrate, which is increased to $k \geq 1400\ s^{-1}$ when including hydrogen tunneling through measured kinetic isotope effects. Assuming Arrhenius behavior for the hydroxylation step provides estimated activation free energies of ≤10 kcal/mol. These results are in agreement with experiments on $P450_{cam}$ cited in ref 92, which suggest that the rate constant for substrate hydroxylation is $\geq 1000\ s^{-1}$ with a free energy activation barrier of ≤13 kcal/mol. Cytochrome P450s are important heme enzymes that metabolize drugs using molecular oxygen to form an iron-oxo intermediate that can activate otherwise inert C−H bonds and lead to their hydroxylation.[1−3] This increases the solubility of the substrates and eases their excretion.[1] Many experiments have been performed to try to trap the catalytically competent iron-oxo species; however these attempts have largely been unsuccessful due to compound 1's transient existence.[2]

It is thought that the rate-determining step of the substrate hydroxylation is a hydrogen atom transfer, or even possibly a proton coupled electron transfer, to the iron-oxo moiety. Tian and Friesner[1] have used unrestricted B3LYP/MM methods with large basis sets and solvation models, with explicit inclusion of the recently determined catalytic water close to the iron-oxo moiety of $P450_{cam}$,[93,94] to investigate the energetics of this step for both doublet and quartet channels of $P450_{BM3}$ (see ref 1 for computational details). Their activation energy of the hydrogen atom transfer to the iron-oxo was determined to be approximately 20 kcal/mol and involves a late transition state. This result is in good agreement with many other quantum chemistry calculations performed on a very large number of P450 systems with different properties including $P450_{cam}$, for example, as seen in a recent review[2] and communication.[93] Considering the recent experimental evidence, this barrier is determined to be too large, suggesting errors in either the proposed mechanism or the DFT models used. It is believed that this discrepancy is due to B3LYP's overestimation of the barrier.

The B3LYP activation free energy of 20 kcal/mol may be corrected using our redox parameters considering that the hydrogen atom transfer is essentially indistinguishable from a proton coupled electron transfer within the resolution of the experiments as well as in computations that do not resort to nonadiabatic electron dynamics. In order to divide the error in the hydrogen atom transfer or proton coupled electron transfer into individual error contributions from electron transfer and proton transfer would require a large database of proton transfer energetics. In a recent paper,[42] we studied both proton coupled electron transfer and electron transfer energetics of various ruthenium redox couples where the latter was extensively compared to experimental results by virtue of a large and diverse

dx.doi.org/10.1021/ct2006693 | J. Chem. TheoryComput. 2012, 8, 442−459

database. Unfortunately, the same kind of study was not possible for the proton coupled electron transfer reactions because there were not nearly as many experimental instances. However, Table 3 of that article shows that for two out of three complexes the difference in B3LYP error with respect to experimental results for proton coupled electron transfer and electron transfer reactions is small, on average at about 0.12 V. There is one large outlier present in that work; however, it is due to the absence of certain electronic states, as predicted by B3LYP/LACV3P, and not a result of the electron transfer being coupled to proton transfer. For this reason, we hypothesize that the errors in hydrogen atom transfers and proton coupled electron transfers are primarily due to errors in B3LYP's treatment of the electron transfer energetics, which for the late transition state presented in Tian and Friesner[1] allows us to apply our new DBLOC redox model.

The atoms that octahedrally coordinate the iron in P450 are (1) oxo (anionic oxygen using the *remss* parameter worth 0.08 V), (2) cys (anionic sulfur using the *relss* parameter worth −0.04 V), (3 and 4) two porphyrin nitrogens (anionic nitrogens using the N^{-1} parameter worth a total of 2(0.16) V), and (5 and 6) two porphyrin nitrogens (aromatic nitrogens using the *remss* parameter worth a total of 2(0.08) V). Therefore, the DBLOC correction for the single-electron reduction becomes 0.5 V (electrochemical framework according to eq 2) or about −11.5 kcal/mol (thermodynamic framework), which brings the activation free energy of around 20 kcal/mol to about 10 kcal/mol, which is much more consistent with Rittle and Green's[3] recent experimental result.

Using B3LYP-D, which is an empirical dispersion correction built upon conventional B3LYP,[95−97] it was recently determined[92] for model complexes that dispersion interactions between the substrate and the porphyrin ring of the heme subunit of cytochrome $P450_{cam}$ may play a role in lowering the activation energies by an average of about 4 kcal/mol. Whether this 4 kcal/mol stabilization in the activation free energy for the model complex is transferable to a QM/MM P450 model, for example, like the Tian and Friesner P450 model that is being considered in this article, depends on if the dispersion correction for the model complex is similar to what would be obtained in a B3LYP-D/MM calculation. The transferability to B3LYP-D/MM calculations may require that B3LYP-D and B3LYP have roughly similar interaction energies with the MM region because, otherwise, dispersion interactions of the heme unit and substrate with the enzyme active site may strongly inhibit the 4 kcal/mol stabilization. While we have found that the dominant error in the P450 hydrogen atom transfer activation free energy is a result of the incorrect electron transfer energetics obtained with B3LYP, there may be smaller error contributions due to dispersion interactions, as well as errors that would be corrected by applying the organic LOC model etc., and we plan to investigate this in future work.

5. CONCLUSION

Using a database of experimental single-electron reduction potentials for 95 diverse octahedral fourth-row transition metal complexes, we were able to extend our previous DBLOC model developed for calculating accurate spin-splitting properties to deliver similar accuracy for B3LYP redox potentials in a continuum solvent. Application of the model reduces the MUE in B3LYP from 0.40 ± 0.20 V (0.88 V max error) to 0.12 ± 0.09 V (0.34 V max error) using seven physical parameters that substantially improve the B3LYP prediction of HOMO/LUMO d-orbital energetics. Like our previous spin-splitting model, the redox parameters correlate with the spectrochemical series, and experimental reduction potentials for the doublet excited state of $[Cr(III)(phen)_3]^{+3}$ have made it possible to properly close a thermodynamic cycle that makes use of both the spin-splitting and redox DBLOC parameters. It was found that B3LYP/LACV3P makes systematic errors in the strength of the metal−ligand bonds in transition metal complexes that manifest themselves in two different physical ways, namely, (1) in predicting by how much the ligands shift the energies of the d orbitals relative to the free metal center where more strongly interacting ligands that lie to the right of the spectrochemical series are strongly overbound, while more weakly interacting ligands that lie to the left of the spectrochemical series are strongly underbound and (2) in predicting the energies of the e_g orbitals relative to the t_{2g} orbitals where for more strongly interacting ligands e_g is strongly overbound while for more weakly interacting ligands e_g is weakly overbound. The new set of redox parameters exhibits the same linear relationship with respect to the spectrochemical series as the spin-splitting parameters but is shifted by an amount that is well within the acceptable level of uncertainty in this work. This suggests that with a higher degree of resolution in both experimental and computational data that the two parameter sets may in fact merge into one small parameter set that is capable of correcting the B3LYP energetics of a very large database of different transition metal complexes.

Spin-crossover complexes present themselves in two different ways in our redox database: (1) spin-crossovers for oxidized and/or reduced complexes and (2) spin-crossovers that are coupled to the reduction process. For the former, application of our previous spin-splitting DBLOC model correctly reverses the ordering of energies of states with different spin-multiplicities which are incorrectly determined by B3LYP due to its overbinding of high spin states. The same spin-splitting parameters may be applied to correct the spin-crossover component of the error for spin-crossover coupled redox reactions where their total contributions are found to be small in comparison to the redox contributions, indicating that it is the redox reaction itself, as opposed to the coupled spin-crossover, that dominates the error for spin-crossover coupled redox reactions.

Recent experimental evidence[3] on the elusive cytochrome P450 compound I indicates that the substrate hydroxylation barrier is around ≤10 kcal/mol, which shows that many previously computed activation energies are on average too high. In agreement with a number of other computational studies,[2,92−94] Tian and Friesner[1] recently estimated the barrier at about 20 kcal/mol using unrestricted B3LYP/MM. Correcting this barrier using our new empirical correction scheme for B3LYP redox potentials reduces it by about 10 kcal/mol and provides significantly better agreement with the recent experimental result.

■ ASSOCIATED CONTENT

Ⓢ Supporting Information

A detailed discussion of the dependence of redox potentials on solution conditions as well as a number of figures showing experimental and calculated data are provided. Cartesian coordinates and pictures of all of the complexes in our redox database are also given. This material is available free of charge via the Internet at http://pubs.acs.org.

AUTHOR INFORMATION

Corresponding Author

*E-mail: rich@chem.columbia.edu.

Notes

The authors declare the following competing financial interest(s): R.A.F. has a significant financial stake in Schrödinger, Inc., is a consultant to Schrödinger, Inc., and is on the Scientific Advisory Board of Schrödinger, Inc.

ACKNOWLEDGMENTS

This work has been supported by the Department of Energy program through solar photochemistry (DE-FG02-90ER-14162) to R.A.F.

REFERENCES

(1) Tian, L.; Friesner, R. A. *J. Chem. Theory Comput.* **2009**, *5*, 1421.
(2) Shaik, S.; Cohen, S.; Wang, Y.; Chen, H.; Kumar, D.; Thiel, W. *Chem. Rev.* **2010**, *110*, 949.
(3) Rittle, J.; Green, M. T. *Science* **2010**, *330*, 933.
(4) Rinaldo, D.; Philipp, D.; Lippard, S.; Friesner, R. *J. Am. Chem. Soc.* **2007**, *129*, 3135.
(5) Concepcion, J. J.; Jurss, J. W.; Brennaman, M. K.; Hoertz, P. G.; Patrocinio, A. O. T.; Iha, N. Y. M.; Templeton, J. L.; Meyer, T. J. *Acc. Chem. Res.* **2009**, *42*, 1954.
(6) Hammes-Schiffer, S. *Acc. Chem. Res.* **2001**, *34*, 273.
(7) Monti, D.; Ottolina, G.; Carrea, G.; Riva, S. *Chem. Rev.* **2011**, *111*, 4111.
(8) Lord, R. L.; Schultz, F. A.; Baik, M.-H. *J. Am. Chem. Soc.* **2009**, *131*, 6189.
(9) Harvey, J. N.; Aschi, M. *Faraday Discuss.* **2003**, *124*, 129.
(10) Graham, J. P. *Inorg. Chim. Acta* **2009**, *362*, 2080.
(11) Moens, J.; De Proft, F.; Geerlings, P. *Phys. Chem. Chem. Phys.* **2010**, *12*, 13174.
(12) Pombeiro, A. J. *J. Organomet. Chem.* **2005**, *690*, 6021.
(13) Pickett, C.; Pletcher, D. *J. Org. Chem.* **1975**, *102*, 327.
(14) Chatt, J.; Kan, C. T.; Leigh, G. J.; Pickett, C. J.; Stanley, D. R. *Dalton Trans.* **1980**, 2032.
(15) Bursten, B. E.; Green, M. R.; Katovic′, V.; Kirk, J. R.; Lightner, D. Jr. *Inorg. Chem.* **1986**, *25*, 831.
(16) Bursten, B. E. *J. Am. Chem. Soc.* **1982**, *104*, 1299.
(17) Lever, A. B. P. *Inorg. Chem.* **1990**, *29*, 1271.
(18) Hall, M. B.; Fenske, R. F. *Inorg. Chem.* **1972**, *11*, 768.
(19) Parr, R. G.; Yang, W. *Density-Functional Theory of Atoms and Molecules*; Oxford University Press, Inc.: New York, 1989.
(20) Pombeiro, A. J. L. *Eur. J. Inorg. Chem.* **2007**, 1473.
(21) Lu, J.; Yaman, A.; Clarke, M. J. *Inorg. Chem.* **1990**, *29*, 3483.
(22) Lever, A. B. P. *Inorg. Chem.* **1991**, *30*, 1980.
(23) Masui, H.; Lever, A. B. P. *Inorg. Chem.* **1993**, *32*, 2199.
(24) Hansch, C.; Leo, A.; Taft, R. W. *Chem. Rev.* **1991**, *91*, 165.
(25) Lee, C.; Yang, W.; Parr, R. *Phys. Rev. B* **1988**, *37*, 785.
(26) Becke, A. *J. Chem. Phys.* **1993**, *98*, 5648.
(27) Hughes, T. F.; Friesner, R. A. *J. Chem. Theory Comput.* **2011**, *7*, 19.
(28) Friesner, R. A.; Knoll, E. H.; Cao, Y. *J. Chem. Phys.* **2006**, *125*, 124107.
(29) Knoll, E. H.; Friesner, R. A. *J. Phys. Chem. B* **2006**, *110*, 18787.
(30) Goldfeld, D.; Bochevarov, A.; Friesner, R. A. *J. Chem. Phys.* **2008**, *129*, 214105.
(31) Hall, M.; Goldfeld, D.; Bochevarov, A.; Friesner, R. A. *J. Chem. Theory Comput.* **2009**, *5*, 2996.
(32) Rinaldo, D.; Tian, L.; Harvey, J.; Friesner, R. A. *J. Chem. Phys.* **2008**, *129*, 164108.
(33) Roy, L. E.; Jakubikova, E.; Guthrie, M. G.; Batista, E. R. *J. Phys. Chem. A* **2009**, *113*, 6745.
(34) Migliore, A.; Sit, P. H.-L.; Klein, M. L. *J. Chem. Theory Comput.* **2009**, *5*, 307.
(35) Uudsemaa, M.; Tamm, T. *J. Phys. Chem. A* **2003**, *107*, 9997.
(36) Baik, M.-H.; Friesner, R. A. *J. Phys. Chem. A* **2002**, *106*, 7407.
(37) Kobayashi, H.; Miura, T.; Shimodaira, Y.; Kudo, A. *Chem. Lett.* **2004**, *33*, 1176.
(38) Galstyan, A.; Knapp, E.-W. *J. Comput. Chem.* **2009**, *30*, 203.
(39) de Groot, M. T.; Koper, M. T. M. *Phys. Chem. Chem. Phys.* **2008**, *10*, 1023.
(40) Shimodaira, Y.; Miura, T.; Kudo, A.; Kobayashi, H. *J. Chem. Theory Comput.* **2007**, *3*, 789.
(41) Srnec, M.; Chalupský, J.; Fojta, M.; Zendlová, L.; Havran, L.; Hocek, M.; Kývala, M.; Rulíšek, L. *J. Am. Chem. Soc.* **2008**, *130*, 10947.
(42) Hughes, T. F.; Friesner, R. A. *J. Phys. Chem. B* **2011**, *115*, 9280.
(43) Pavlishchuk, V. V.; Addison, A. W. *Inorg. Chim. Acta* **2000**, *298*, 97.
(44) Milazzo, G.; Caroli, S. *Tables of Standard Electrode Potentials*; John Wiley & Sons, Ltd.: New York, 1978.
(45) Bard, A. J.; Parsons, R.; Jordan, J. *Standard Potentials in Aqueous Solution*; Marcel Dekker, Inc.: New York, 1985.
(46) Guldi, D.; Wasgestian, F.; Meyerstein, D. *Inorg. Chim. Acta* **1992**, *194*, 15.
(47) Krüger, H.-J.; Holm, R. H. *J. Am. Chem. Soc.* **1990**, *112*, 2955.
(48) De Alwis, D. C. L.; Schultz, F. A. *Inorg. Chem.* **2003**, *42*, 3616.
(49) Siburt, C. J. P.; Lin, E. M.; Brandt, S. J.; Tinoco, A. D.; Valentine, A. M.; Crumbliss, A. L. *J. Inorg. Biochem.* **2010**, *104*, 1006.
(50) Ward, M. S.; Shepherd, R. E. *Inorg. Chim. Acta* **1999**, *286*, 197.
(51) Banerjee, P.; Sproules, S.; Weyhermüller, T.; George, S. D.; Wieghardt, K. *Inorg. Chem.* **2009**, *48*, 5829.
(52) Wharton, E. J.; McCleverty, J. A. *J. Chem. Soc. A* **1969**, 2258.
(53) Sproules, S.; Weyhermüller, T.; DeBeer, S.; Wieghardt, K. *Inorg. Chem.* **2010**, *49*, 5241.
(54) Krüger, H.-J.; Peng, G.; Holm, R. H. *Inorg. Chem.* **1991**, *30*, 734.
(55) Kotov, V. Y.; Nazmutdinov, R. R.; Botukhova, G. N.; Tsirlina, G. A.; Petrii, O. A. *Mendel. Commun.* **2004**, *3*, 113.
(56) Fronaeus, S.; Berglund, J.; Elding, L. I. *Inorg. Chem.* **1998**, *37*, 4939.
(57) Groni, S.; Hureau, C.; Guillot, R.; Blondin, G.; Blain, G.; Anxolabéhère-Mallart, E. *Inorg. Chem.* **2008**, *47*, 11783.
(58) Hecht, M.; Schultz, F. A.; Speiser, B. *Inorg. Chem.* **1996**, *35*, 5555.
(59) Basallote, M. G.; Bernhardt, P. V.; Calvet, T.; Castillo, C. E.; Font-Bardia, M.; Martínez, M.; Rodríguez, C. *Dalton Trans.* **2009**, 9567.
(60) Sjödin, M.; Gätjens, J.; Tabares, L. C.; Thuéry, P.; Pecoraro, V. L.; Un, S. *Inorg. Chem.* **2008**, *47*, 2897.
(61) Brausam, A.; Maigut, J.; Meier, R.; Szilágyi, P. A.; Buschmann, H.-J.; Massa, W.; Homonnay, Z.; van Eldik, R. *Inorg. Chem.* **2009**, *48*, 7864.
(62) Walsh, J. H.; Earley, J. E. *Inorg. Chem.* **1964**, *3*, 343.
(63) Sharpe, P.; Richardson, D. E. *J. Am. Chem. Soc.* **1991**, *113*, 8339.
(64) Da Luz, D.; Franco, C. V.; Vencato, I.; Neves, A.; Mascarenhas, Y. P. *J. Coord. Chem.* **1992**, *26*, 269.
(65) Pecsok, R. L.; Shields, L. D.; Schaefer, W. P. *Inorg. Chem.* **1964**, *3*, 114.
(66) Tanaka, N.; Tomita, T.; Yamada, A. *Bull. Chem. Soc. Jpn.* **1970**, *43*, 2042.
(67) Tanaka, N.; Ogino, H. *Bull. Chem. Soc. Jpn.* **1965**, *38*, 1054.
(68) Schaefer, W. P. *Inorg. Chem.* **1965**, *4*, 642.
(69) Ogino, H.; Ogino, K. *Inorg. Chem.* **1983**, *22*, 2208.
(70) Murray, R. C. Jr.; Rock, P. A. *Electrochim. Acta* **1968**, *13*, 969.
(71) Hume, D. N.; Kolthoff, I. M. *J. Am. Chem. Soc.* **1943**, *65*, 1897.
(72) Fu, Y.; Cole, A. S.; Swaddle, T. W. *J. Am. Chem. Soc.* **1999**, *121*, 10410.
(73) Chambers, J.; Eaves, B.; Parker, D.; Claxton, R.; Ray, P. S.; Slattery, S. J. *Inorg. Chim. Acta* **2006**, *359*, 2400.
(74) Hecht, M.; Fawcett, W. R. *J. Phys. Chem.* **1996**, *100*, 14240.
(75) McDaniel, A. M.; Tseng, H.-W.; Damrauer, N. H.; Shores, M. P. *Inorg. Chem.* **2010**, *49*, 7981.
(76) *Jaguar*, version 7.5; Schrödinger, Inc.: New York.
(77) Hay, P. J.; Wadt, W. R. *J. Chem. Phys.* **1985**, *82*, 299.
(78) Allen, F. H. *Acta Crystallogr.* **2002**, *B58*, 380.

(79) Vacek, G.; Perry, J. K.; Langlois, J.-M. *Chem. Phys. Lett.* **1999**, *310*, 189.
(80) Swart, M. *Inorg. Chim. Acta* **2007**, *360*, 179.
(81) Robbins, J. L.; Edelstein, N.; Spencer, B.; Smart, J. C. *J. Am. Chem. Soc.* **1982**, *104*, 1882.
(82) Meier, R. M.; Hanusa, T. P. *Encyclopedia of Inorganic Chemistry, Symmetry and Steric Effects on Spin States in Transition Metal Complexes*; 2011.
(83) Gutlich, P.; Hauser, A.; Spiering, H. *Angew. Chem., Int. Ed. Engl.* **1994**, *33*, 2024.
(84) Reiher, M. *Inorg. Chem.* **2002**, *41*, 6928.
(85) Farina, R.; Wilkins, R. G. *Inorg. Chem.* **1968**, *7*, 514.
(86) Wangila, G. W.; Jordan, R. B. *Inorg. Chim. Acta* **2005**, *358*, 3753.
(87) Ochiai, E. *Bioinorganic Chemistry: A Survey*; Elsevier, Inc.: Amsterdam, 2008.
(88) Salomon, O.; Reiher, M.; Artur Hess, B. *J. Chem. Phys.* **2002**, *117*, 4729.
(89) Serpone, N.; Jamieson, M. A.; Henry, M. S.; Hoffman, M. Z.; Bolletta, F.; Maestri, M. *J. Am. Chem. Soc.* **1979**, *101*, 2907.
(90) Gsponer, H.; Argüello, G. A.; Argüello, G. A.; Staricco, E. H. *Inorg. Chim. Acta* **1991**, *189*, 207.
(91) Isaacs, M.; Sykes, A. G.; Ronco, S. *Inorg. Chim. Acta* **2006**, *359*, 3847.
(92) Lonsdale, R.; Harvey, J. N.; Mulholland, A. J. *J. Phys. Chem. Lett.* **2010**, *1*, 3232.
(93) Altun, A.; Guallar, V.; Friesner, R. A.; Shaik, S.; Thiel, W. *J. Am. Chem. Soc.* **2006**, *128*, 3924.
(94) Altun, A.; Shaik, S.; Thiel, W. *J. Comput. Chem.* **2006**, *27*, 1324.
(95) Grimme, S. *J. Comput. Chem.* **2006**, *27*, 1787.
(96) Grimme, S. *J. Comput. Chem.* **2004**, *25*, 1463.
(97) Schneebeli, S. T.; Bochevarov, A. D.; Friesner, R. A. *J. Chem. Theory Comput.* **2011**, *7*, 658.